The Role of Cloud Radiative Heating in Determining the Location of the ITCZ in Aquaplanet Simulations

Bryce E. Harrop and Dennis L. Hartmann

Department of Atmospheric Sciences, University of Washington, Seattle, Washington

(Manuscript received 24 July 2015, in final form 20 January 2016)

ABSTRACT

The relationship between the tropical circulation and cloud radiative effect is investigated. Output from the Clouds On–Off Klimate Intercomparison Experiment (COOKIE) is used to examine the impact of cloud radiative effects on circulation and climate. In aquaplanet simulations with a fixed SST pattern, the cloud radiative effect leads to an equatorward contraction of the intertropical convergence zone (ITCZ) and a reduction of the double ITCZ problem. It is shown that the cloud radiative heating in the upper troposphere increases the temperature, weakens CAPE, and inhibits the onset of convection until it is closer to the equator, where SSTs are higher. Precipitation peaks at higher values in a narrower band when the cloud radiative effects are active, compared to when they are inactive, owing to the enhancement in moisture convergence. Additionally, cloud–radiation interactions strengthen the mean meridional circulation and consequently enhance the moisture convergence. Although the mean tropical precipitation decreases, the atmospheric cloud radiative effect has a strong meridional gradient, which supports stronger poleward energy flux and speeds up the Hadley circulation. Cloud radiative heating also enhances cloud water path (liquid plus ice), which, combined with the reduction in precipitation, suggests that the cloud radiative heating reduces precipitation efficiency in these models.

1. Introduction and background

The intertropical convergence zone (ITCZ) describes zonally oriented bands of heavy precipitation in the tropics where surface winds converge. The ITCZ is important for the precipitation, but it is also a critical factor in simulating the global energy and moisture distributions and transports, as well as the tropical top-of-atmosphere and surface fluxes. Its location has a strong impact on the trade winds and ocean circulation. On average, Earth has a single ITCZ across the tropical Pacific that is displaced into the Northern Hemisphere. While a secondary ITCZ is occasionally observed in the southern Pacific, it is a transient phenomenon occurring primarily in boreal spring (Hubert et al. 1969; Zhang 2001). Coupled climate models, however, often show a second ITCZ in the Southern Hemisphere in the climatological mean rainfall patterns (see, e.g., Mechoso et al. 1995; Lin 2007; Flato et al. 2013; Li and Xie 2014). This unrealistic secondary ITCZ is often referred to as the double ITCZ problem. Tian (2015) showed that the double ITCZ bias negatively correlates with equilibrium climate sensitivity (ECS); ECS is higher in models with a weaker bias.

Double ITCZ features are not restricted to coupled models alone and have been shown to exist even in aquaplanet simulations with fixed sea surface temperature patterns (Numaguti 1993; Barsugli et al. 2005; Liu and Moncrieff 2008; Liu et al. 2010; Dahms et al. 2011; Möbis and Stevens 2012; Oueslati and Bellon 2013a,b; Landu et al. 2014). Across many studies, a variety of factors have been shown capable of shifting a model from a single to double ITCZ. Examples include changing the model resolution (Landu et al. 2014), removing wind contributions to surface evaporation (Numaguti 1993), changing convective parameterizations (Numaguti 1993; Liu et al. 2010; Möbis and Stevens 2012; Oueslati and Bellon 2013a), changing the SST gradient (Dahms et al. 2011; Oueslati and Bellon 2013b), using homogenized radiative cooling (Liu and Moncrieff 2008), and even changing the solar constant (Barsugli et al. 2005).

Chao and Chen (2004) summarized the ITCZ position as the sum of two "attractors." The first attractor pulls the ITCZ toward the equator according to wave stability arguments, while the second attractor pulls the ITCZ poleward following arguments based on circulation

Corresponding author address: Bryce E. Harrop, Dept. of Atmospheric Sciences, University of Washington, Box 351640, Seattle, WA 98195-1640.
E-mail: beharrop@u.washington.edu

DOI: 10.1175/JCLI-D-15-0521.1

© 2016 American Meteorological Society

strength and surface turbulent energy fluxes. Circulation strength is an important component to the surface fluxes through a positive feedback whereby stronger circulations drive faster winds, thereby picking up more latent and sensible heat from the surface to supply to the convection. Only the second of these attractors depends on model parameters. We suggest that the cloud radiative heating behaves like the first attractor, enhancing convection near the equator. Chao and Chen (2004), however, performed an experiment where the cloud–radiation interactions were removed and compared it to one where they were not and found the ITCZ locations to be roughly unchanged. Their experiments were performed in an aquaplanet model with globally uniform sea surface temperature. Unlike the experiments of Chao and Chen (2004), the experiments examined in this manuscript have an SST distribution with a maximum at the equator. The SST distribution, as we will note again later, is an important component to the difference in our results and those of Chao and Chen (2004).

As noted above, we suggest that the cloud radiative heating within the atmosphere is also an attractor for the ITCZ to be closer to the equator, which is also the region of warmest sea surface temperature (SST) in the experiments described. The cloud radiative heating warms the atmosphere substantially, requiring higher near-surface moist static energy (MSE) values in order to initiate deep convection. This is the same idea as the ''upped ante'' mechanism described by Neelin et al. (2003)—in a warmer atmosphere, higher boundary layer MSE is required for convection. A similar idea was presented by Landu et al. (2014) based upon arguments pertaining to CAPE, and we will use this CAPE approach in our analysis. We will perform our analysis for six models: those used in the Clouds On–Off Klimate Intercomparison Experiment (COOKIE; see Stevens et al. 2012). We will use the aquaplanet simulations from COOKIE. Aquaplanet simulations offer an attractive test bed for learning about the atmosphere due to their removal of Earth's irregularities (Lorenz 1967; Hoskins et al. 1999; Miura et al. 2005; Medeiros et al. 2008, 2015). Removing the landmasses is especially attractive for exploring the relation between clouds and the tropical circulation because land–ocean temperature contrasts may exert a significant influence on the circulation patterns. Using the aquaplanet simulations from COOKIE removes these complexities from consideration, yielding a simpler experiment. Crueger and Stevens (2015) showed a preference for a double ITCZ when cloud–radiation interactions are removed in the COOKIE atmosphere-only models (fixed sea surface temperature experiments with realistic geography), although they do not offer a physical mechanism for this phenomenon.

Cloud radiative heating is an important component of the tropical circulation (see Ramanathan 1987; Slingo and Slingo 1988, 1991; Stuhlmann and Smith 1988a,b; Randall et al. 1989; Sherwood et al. 1994; Zhang and Rossow 1997; Sohn 1999; Bergman and Hendon 2000a,b; Raymond 2000; Tian et al. 2001; Tian and Ramanathan 2002, 2003; Lee and Yoo 2014; Del Genio and Chen 2015; Crueger and Stevens 2015; Harrop and Hartmann 2015; Merlis 2015). Other studies have suggested a role for local cloud radiative heating in determining the ITCZ position. Voigt et al. (2014) showed that the spread in model ITCZ shift is related to the tropical cloud radiative heating. Because climate models tend to have varied responses in how their clouds change with warming (either a prescribed SST increase or by CO_2 forcing), the corresponding change in circulation due to the new heating patterns varies strongly from model to model as well. Voigt and Shaw (2015) showed similar results from aquaplanet simulations. They noted that in global warming experiments, cloud radiative heating led to a latitudinal contraction of precipitation in one model but an expansion of precipitation in another.

Another example of a local tropical effect was considered by Li and Xie (2014), who found the lack of snow–radiation interactions a means for influencing the eastward overextension of the SPCZ seen in the CMIP models. In addition, Raymond (2000) showed that differential cloud radiative heating is fundamental for the tropical circulations. Raymond (2000) also showed that precipitation remains over the warmest SSTs when cloud radiative heating is removed—opposite to what we find here—although the distribution of precipitation widens. Wofsy and Kuang (2012) showed that the warm pool [defined as the precipitating region within their cloud-resolving model (CRM)] narrows as radiative cooling increases in magnitude. They explain this as a response of the increase in precipitation needed to balance the increase in radiative cooling favoring the warmest SSTs.

Despite the models used in COOKIE having different resolutions, different dynamics, different physical parameterizations, and, ultimately, different climates, their ITCZ responses to the removal of the radiative effects of clouds are consistent. Our results confirm the increase in precipitation and circulation strength when cloud radiative effects are included, at least locally. Across the whole of the tropics, however, total precipitation decreases when cloud radiative effects are included, owing to the reduced radiative cooling of the troposphere. We also show that cloud radiative effects constrain the ITCZ to be nearer the equator than when the cloud radiative effects on the atmosphere are removed. The narrowing of convection toward the warmest SSTs agrees with simulations

TABLE 1. Model descriptions and details. (Expansions of acronyms are available online at http://www.ametsoc.org/PubsAcronymList.)

Modeling center	Model name	Model abbreviation for this study	Gridpoint resolution (lon × lat)	Citations	Comments
Centre National de Recherches Météorologiques (CNRM)	CNRM-CM5.1	CNRM	256 × 128 (1.41° × 1.40°)	Voldoire et al. (2013)	—
Geophysical Fluid Dynamics Laboratory (GFDL)	GFDL Atmospheric Model, version 2.1 (AM2.1)	GFDL	144 × 90 (2.5° × 2°)	Anderson et al. (2004)	Not part of original COOKIE
Met Office Hadley Centre (MOHC)	HadGEM2-A	HadGEM	192 × 145 (1.875° × 1.25°)	Collins et al. (2008)	—
Institute Pierre-Simon Laplace (IPSL)	IPSL-CM5A-LR	IPSL-A	96 × 96 (3.75° × 1.89°)	Dufresne et al. (2013), Hourdin et al. (2013a)	Physics package version A
	IPSL-CM5B-LR	IPSL-B	96 × 96 (3.75° × 1.89°)	Dufresne et al. (2013), Hourdin et al. (2013b)	Physics package version B
Max Planck Institute for Meteorology (MPI-M)	ECHAM6	MPI	192 × 96 (1.875° × 1.8653°)	Stevens et al. (2013)	—
Meteorological Research Institute (MRI)	MRI-CGCM3	MRI	320 × 160 (1.125° × 1.12°)	Yukimoto et al. (2012)	—

done by Randall et al. (1989) where cloud radiative heating was turned on and off, and with simulations done by Liu and Moncrieff (2008) where radiative heating was interactive or a fixed, uniform value. Additionally, strong local precipitation rates and vertical velocities are more likely when cloud radiative heating is present. While cloud radiative heating reduces precipitation across the tropics, it increases cloud mass (both liquid and ice), suggesting that cloud radiative heating decreases precipitation efficiency. We find that although precipitation in the tropics is reduced, the mass circulation of the Hadley cell increases. One reason for this is that while the atmospheric cloud radiative effect (ACRE) causes the static stability of the tropics to increase, ACRE also heats the tropical atmosphere and cools the extratropical atmosphere. The enhanced meridional heating gradient drives a stronger poleward heat flux, strengthening the Hadley circulation.

2. Model description and methods

The aquaplanet simulations follow the methodology of the Aqua-Planet Experiment (APE) project. The motivation and experimental design for APE was initially put forth by Neale and Hoskins (2000). The sea surface temperatures are fixed at the Qobs profile from APE. There are six companion experiments done, each with an ACRE-on and ACRE-off configuration; ACRE-on refers to simulations where the cloud–radiation interactions are incorporated and ACRE-off refers to simulations where the cloud–radiation interactions are removed. All of the models output five years of data with both ACRE-on and ACRE-off configurations. While all of the models output monthly data, only a subset output daily data. Thus, for consistency, we will use the monthly data output in this study, except where specifically noted. Because the aquaplanet simulation boundary conditions have no zonal asymmetries, we zonally average all of the model outputs. Five different models are available, with one using two different physics packages (see Table 1 for details). The models are HadGEM (Collins et al. 2008), CNRM (Voldoire et al. 2013), IPSL (Dufresne et al. 2013), MPI (Stevens et al. 2013), and MRI (Yukimoto et al. 2012). The IPSL model is run with two different physics packages which are denoted as IPSL-A and IPSL-B (see Hourdin et al. 2013a,b, respectively). We also perform another aquaplanet experiment with the GFDL model to study the transient response to cloud effect removal.

In addition to the GCMs listed in Table 1, we use the System for Atmospheric Modeling (SAM), version 6.9, cloud-resolving model (Khairoutdinov and Randall 2003). The model uses the anelastic equations of motion. Our model setup has a 3072 × 1 horizontal domain with 1-km resolution and periodic boundary conditions. There are 96 vertical levels on a stretched grid. The upper boundary condition is a rigid lid with Newtonian damping in the upper third of the model domain to limit wave reflection. The prognostic variables in the CRM are liquid-ice water static energy, total nonprecipitating water (water vapor and cloud liquid and ice), and total precipitating water (rain, snow, and graupel). We use the Rapid Radiative Transfer Model for GCMs (RRTMG)

for all of the radiation calculations (see Mlawer et al. 1997; Iacono et al. 2008). All simulations are run to radiative–convective equilibrium. The simulations are run at the equator so there are no rotation effects. We use a perpetual solar forcing with an insolation-weighted solar zenith angle following Hartmann (1994). The ozone profile used in SAM is the tropical profile used in Harrop and Hartmann (2012). We use the base SAM single-moment microphysics scheme as well as a modified microphysics scheme. The modified microphysics scheme is the NOSEDAALIQ5 modification from Lopez et al. (2009). The NOSEDAALIQ5 modifications remove cloud ice sedimentation, lower the threshold for ice autoconversion by a factor of 100, and increase autoconversion and accretion of liquid by factors of 5. For convenience, we will refer to the base SAM microphysics as SAM and the modified microphysics as NA5. Since the cloud-resolving model is a limited domain study, we do not use the same SST pattern as the COOKIE aquaplanet models. Instead, we use a simple cosine distribution of SSTs with amplitude of 1 K and mean of 299 K for all of the simulations. This SST variation is similar in magnitude within the tropics to the Qobs profile used by the COOKIE models.

3. Results and discussion

a. *The influence of stability on precipitation location*

Zonally and temporally averaged precipitation values show an equatorward contraction in the peak precipitation for all simulations when the cloud radiative effects are included (see Fig. 1). We measure the contraction in ITCZ with the precipitation-weighted latitude, calculated as follows:

$$\phi_P = \frac{\int_{0^\circ}^{\phi_{P=\min}} P\phi\cos\phi\, d\phi}{\int_{0^\circ}^{\phi_{P=\min}} P\cos\phi\, d\phi}, \qquad (1)$$

where P is precipitation, ϕ is latitude, and $\phi_{P=\min}$ is the latitude in the Northern Hemisphere where the subtropical minimum in precipitation occurs (typically somewhere between 15° and 30°N in these aquaplanet simulations). Because the models are hemispherically symmetric, we integrate only in one hemisphere; otherwise, ϕ_P would be zero in all of the models. The precipitation-weighted latitude effectively captures the spread of precipitation around the equator. The spread in ITCZ contractions is about 0.5°–3.5° latitude across the models (see Table 2). Note that ϕ_P in the ACRE-on simulation is uncorrelated with $\Delta\phi_P$ (the difference between ACRE-on and ACRE-off simulations).

Figure 2 shows the zonal-mean ACRE values for the six COOKIE models. There is a very strong similarity between ACRE and precipitation, which is not surprising since both are linked by convection. ACRE is positive for all of these models, meaning the clouds are heating the atmospheric column in total. Positive ACRE is expected for tropical high clouds (see Slingo and Slingo 1988), and Fig. 3 (left) shows that high clouds dominate at low latitudes for these models. Figure 3 (right) shows how the cloud fraction responds to the cloud–radiation interactions. Despite only four of the models reporting cloud fraction on the vertical grid, we see a lot of disparity between the model cloud responses. In general, there tends to be more clouds at low latitudes with ACRE-on, but there are a lot of changes in vertical structure that are not consistent between models. It is beyond the scope of this paper to address the vertical structure of changes in cloud amount, but this should be investigated in future work.

Our hypothesis that ACRE contracts the ITCZ equatorward builds on the CAPE argument presented in Landu et al. (2014). The fact that some models use convective quasi equilibrium (CQE) in their convective parameterizations should not preclude the use of CAPE as a guide for the ITCZ contraction in these models. CQE, as described by Arakawa and Schubert (1974), is based on a plume model, which makes use of buoyancy. CAPE is similar to column-integrated buoyancy, so it should be an effective metric for determining where the GCMs produce convection. Landu et al. (2014) proposed that high CAPE values away from the equator favor a double ITCZ, while high CAPE values constrained near the equator favor a single ITCZ. We hypothesize that the equatorward contraction in the ITCZ is driven by changes in CAPE due to the cloud radiative heating. Specifically, the increase in upper tropospheric temperature associated with the cloud radiative heating strengthens the stability and weakens CAPE across the tropics. Therefore, we next verify that the upper tropospheric temperature increases from the ACRE-off to the ACRE-on simulations, despite the fixed sea surface temperatures (see Fig. 4).

As expected, the tropical upper troposphere is warmer in the ACRE-on simulations than in the ACRE-off simulations across all models because of the strong radiative warming of the high clouds. The surface air temperatures do not show much change, which is also to be expected considering that the sea surface temperatures are fixed in all of the simulations. The stratosphere is cooler in the ACRE-on simulations compared to the ACRE-off simulations. This may be due to high clouds trapping longwave fluxes emitted by the lower troposphere from making it into the stratosphere and

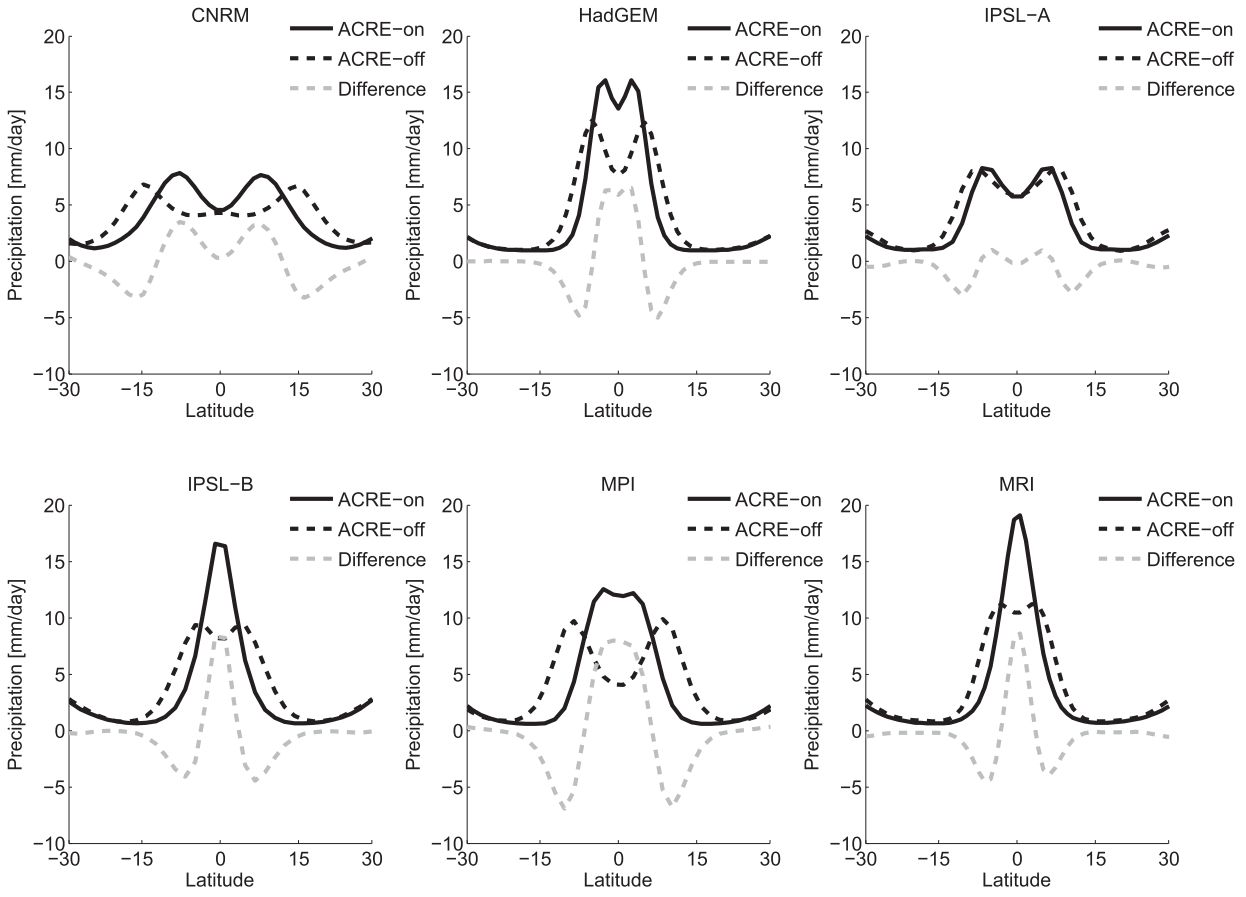


FIG. 1. Precipitation for the six different models. The gray dashed line shows the difference between the ACRE-on and ACRE-off experiments.

causing warming, or it may be due to an increase in the Brewer–Dobson circulation. Indeed the radiative cooling is weaker in the tropical stratosphere with ACRE on (not shown) and the globally averaged stratospheric temperature is also colder with ACRE on, suggesting that there is a radiative impact. However, it is also the case that the high-latitude stratosphere is warmer (not shown), suggesting that there is also a dynamical component. Thus, it is likely that both the radiative and dynamic effects are important for determining the impact of ACRE on the stratosphere, but it is beyond the scope of this paper to quantify these effects. The atmospheric cloud radiative effect also acts to lower the tropopause temperature (not shown). Later we will show that ACRE has a strong latitude gradient from heating in the tropics to cooling in high latitudes, which would drive a stronger circulation.

Cloud–radiation interactions warm the upper tropical troposphere more than lower in the atmosphere and therefore they increase the stability. The ACRE-driven change in stability can be easily quantified as a change in convective available potential energy (CAPE). As noted above, CAPE is an attractive measure of how favorable the environment is for convection. We make use of George Bryan's script to calculate CAPE (freely available from his web page, http://www2.mmm.ucar.edu/people/bryan/; see also Bryan and Fritsch 2004). When the cloud radiative effects are turned on, two things occur: nonzero values of CAPE occur at lower

TABLE 2. Change in tropical precipitation (ACRE-on minus ACRE-off), precipitation-weighted latitude for ACRE-on, and change in precipitation-weighted latitude (ACRE-on minus ACRE-off) for the six COOKIE simulations and the additional run using the GFDL model; ΔPrecipitation is calculated over 30°S–30°N.

Model	ΔPrecipitation (mm day^{-1})	ACRE-on ϕ_P	ϕ_P
CNRM	−0.061	9.58°	−3.29°
GFDL	−0.076	8.03°	−1.27°
HadGEM	−0.011	4.37°	−1.36°
IPSL-A	−0.51	7.23°	−0.44°
IPSL-B	−0.35	4.22°	−2.00°
MPI	−0.14	5.19°	−3.60°
MRI	−0.29	3.94°	−1.13°

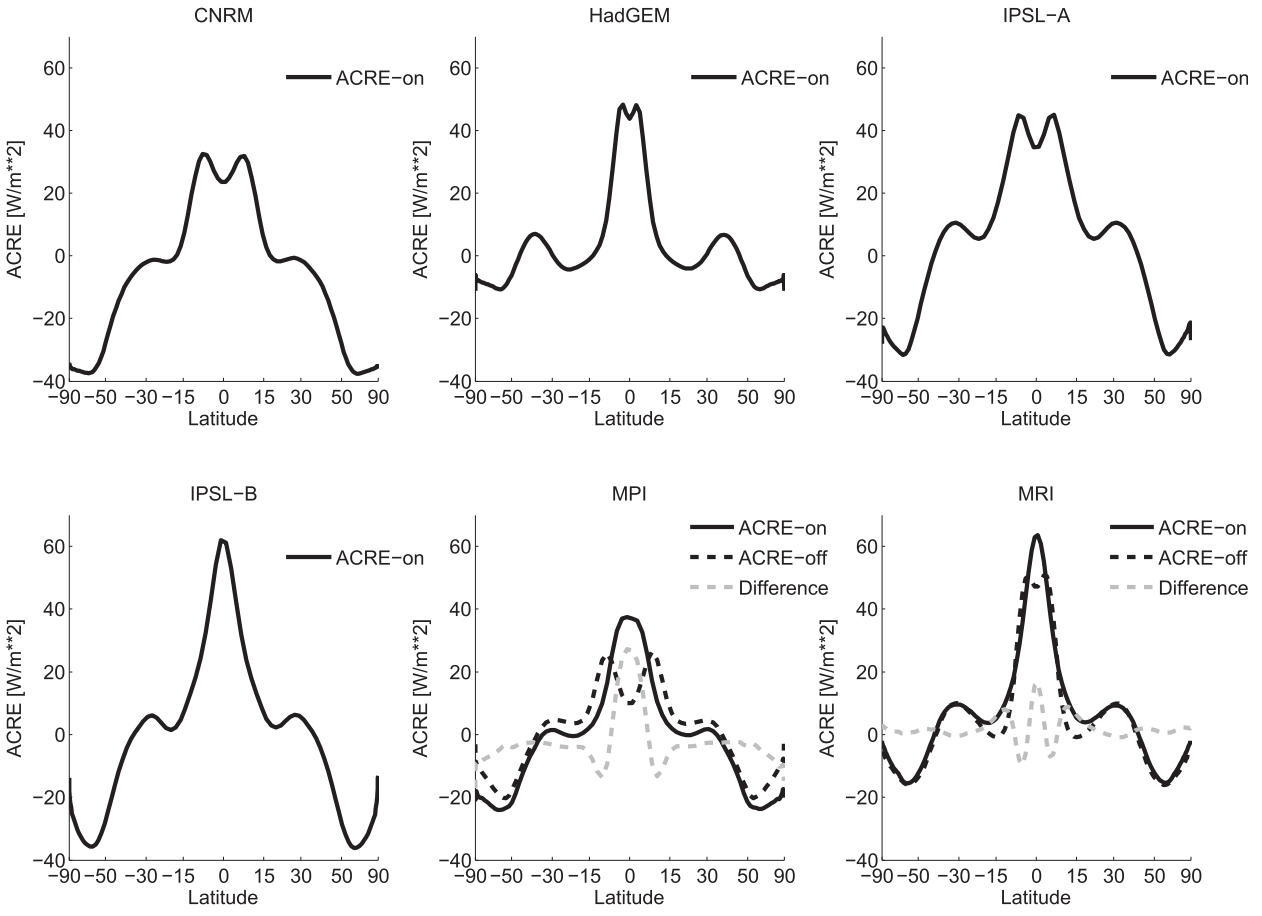


FIG. 2. ACRE for the six different models. The gray dashed line shows the difference between the ACRE-on and ACRE-off experiments. Note that for ACRE-off, the ACRE values reported are those that would occur if cloud–radiation interactions were included in the model. Only MPI and MRI report these ACRE-off values. Note that the latitude range for these figures extends to the poles.

latitudes than in the ACRE-off configuration in all models, and CAPE decreases throughout the whole tropics in all models except CNRM (see Fig. 5). Sherwood et al. (1994) also found that CAPE decreased when cloud radiative effects were included in a climate model.

Temperature changes are not the only means by which CAPE can be changed. Increases in moisture within the boundary layer will increase CAPE, all else being equal. We examine the changes in specific humidity in Fig. 6. We find that including the cloud radiative heating increases the water vapor content of the tropical troposphere. The increase is most prominent right at the equator. Thus, we have competing influences. The clouds, through their radiative heating, act to stabilize the tropical atmosphere and decrease CAPE while at the same time increasing CAPE through increases in moisture—via increases in circulation strength, as we will show later.

As shown in Fig. 5, including ACRE decreases CAPE for five of the six models examined in this study. That alone would suggest that the temperature increase due to ACRE is a stronger influence on the CAPE than the moisture increase, since increases in moisture would lead to an increase in CAPE, all else being equal. We want to know, however, whether the contracting CAPE profile is driven more by changes in temperature or water vapor. To answer this, we recalculate the CAPE using the temperature output from the ACRE-on experiment and the moisture output from the ACRE-off experiment, and vice versa. These terms allow us to compare changes in CAPE due to temperature or moisture alone. If temperature is driving the contraction of the ITCZ, we expect the meridional extent of the CAPE profile for T on–q off to match that of ACRE-on and T off–q on to match that of ACRE-off. If instead moisture is driving the contraction of the CAPE profile, the reverse should be true (i.e., the meridional extent of T off–q on should match ACRE-on). Figure 5 shows temperature changes are the primary driver of the equatorward contraction of CAPE when the clouds

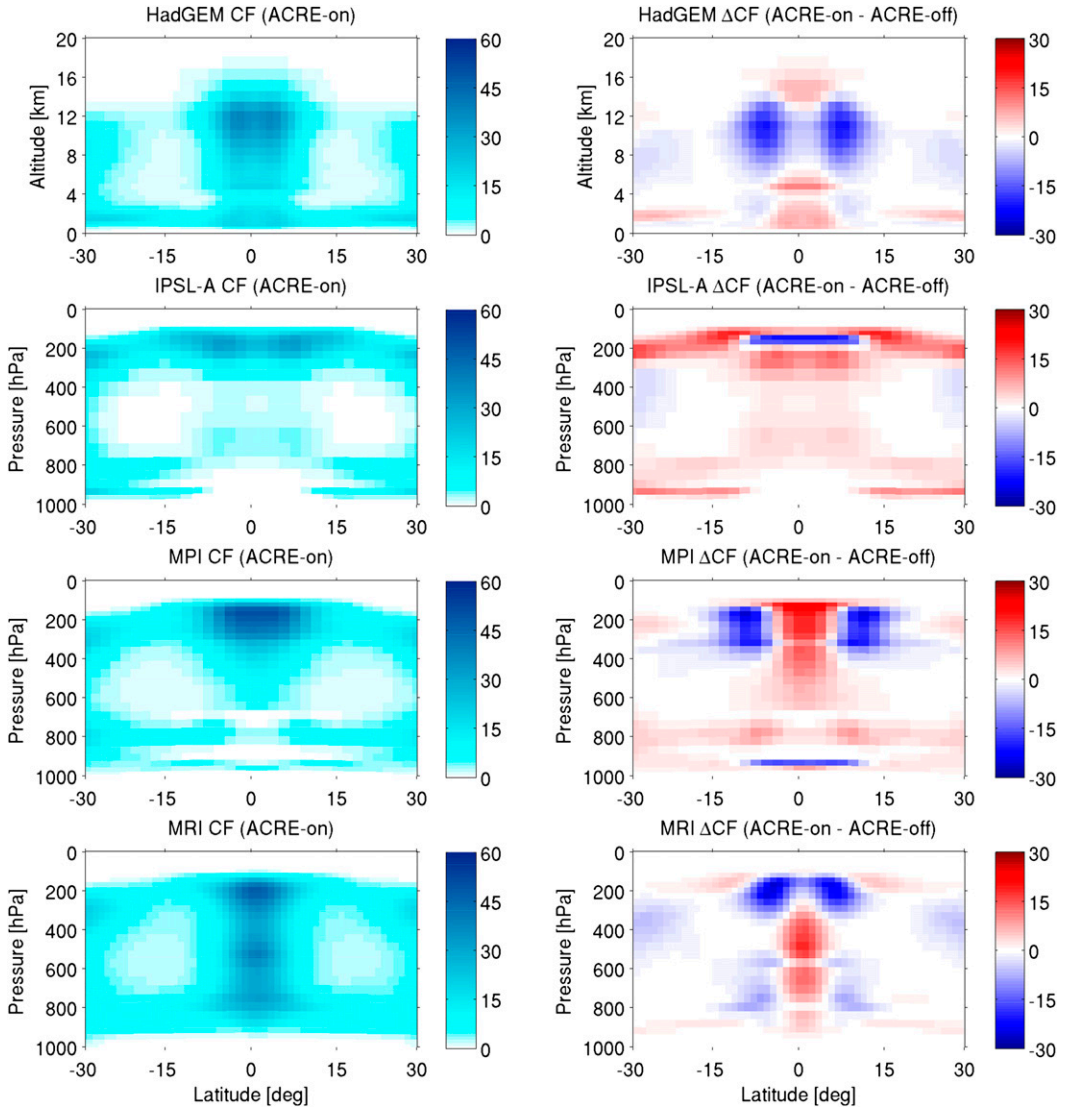


FIG. 3. (left) Zonal-mean cloud fraction (CF) as a function of latitude and altitude or pressure (top)–(bottom) for the four models that report it (HadGEM, IPSL-A, MPI, and MRI). (right) Differences in CF (ACRE-on minus ACRE-off). Amounts and changes are given as a percentage.

are radiatively active. Note that while the meridional structure of the CAPE at low latitudes follows the moisture changes, the meridional extent follows the temperature changes. Since we are interested in the meridional extent of the precipitation, the meridional extent of CAPE is the important factor, and Fig. 5 shows this is determined by the temperature, not the moisture. Even if we scale all of the CAPE profiles to have a peak value of one (not shown), we arrive at the same conclusion that temperature is the dominant control on the meridional extent of the CAPE profile. The CNRM model has a different behavior than the other five models. Not only do the moisture changes between the ACRE-on and ACRE-off experiments in CNRM dominate the CAPE response, they also contribute some to the equatorward contraction of CAPE.

We attempted to identify a correlation between the magnitude of the cloud radiative heating in the ACRE-on experiments and the magnitude of the poleward movement of the ITCZ when the cloud radiative effect is removed, but no such relationship was significant. There is only a weak correlation ($r = -0.6$) between the change in upper tropospheric temperature and the magnitude of the decrease in the precipitation-weighted latitude, so other factors (e.g., latent heat flux, wind speed, eddy fluxes, and mean-state temperature and humidity) must play a nontrivial role for determining any given model's exact ITCZ position. This is, of course, not surprising.

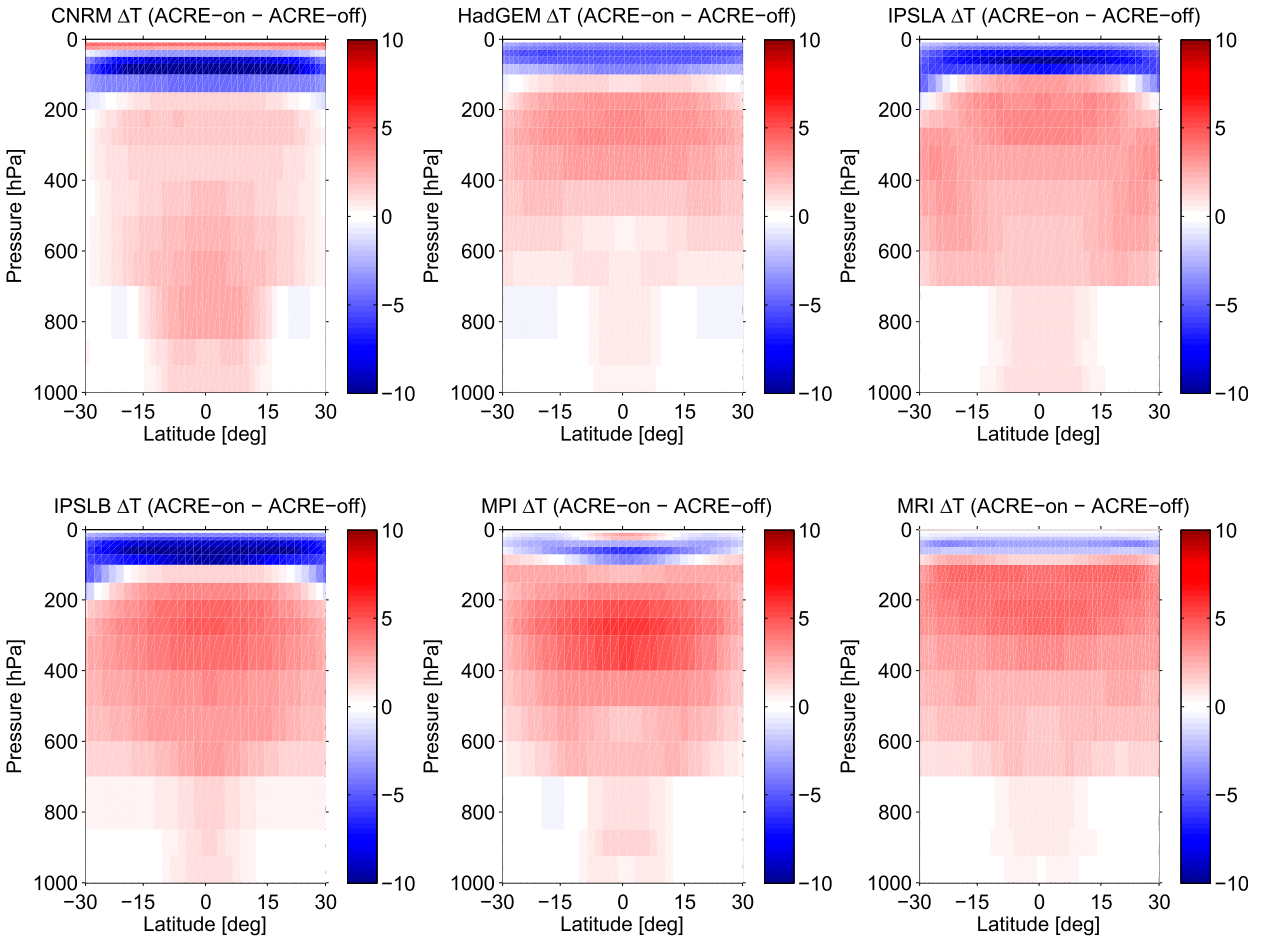


FIG. 4. Difference in air temperature (K) caused by the cloud radiative effect for all six COOKIE models.

We have shown that the cloud radiative heating is responsible for keeping the ITCZ closer to the equator than it would be without that cloud radiative heating, but why is it closer? Why does the ITCZ not simply match the CAPE profile in width and structure? We will expand on the hypothesis presented in Landu et al. (2014) suggesting that the convective bands prevent moisture convergence equatorward of their latitude. In other words, the moisture convergence from the subtropics to the tropics only penetrates as far as the ITCZs. The equation for the moisture budget is

$$\frac{\partial w}{\partial t} + \nabla \cdot \frac{1}{g} \int_0^{p_s} q\mathbf{v}\, dp = E - P, \tag{2}$$

where g is the gravitational acceleration constant, p_s is the surface pressure, $\mathbf{v}$ is the horizontal velocity, w is the precipitable water, q is the specific humidity, E is the surface evaporation, and P is the surface precipitation. The second term on the right is the moisture divergence. From Landu et al. (2014), we expect the moisture convergence to be weaker at the equator when the cloud radiative effects are turned off, and indeed that is the case. As expected, the changes in moisture convergence are strikingly similar to those seen in precipitation above (not shown). We have compared our calculations of moisture convergence using monthly data to those using daily data for the models that have daily data available and find little difference between them.

It is common in the literature for changes in surface fluxes to be responsible for switching between single and double ITCZs within models (e.g., Numaguti 1993; Barsugli et al. 2005; Möbis and Stevens 2012; Liu et al. 2010). While we have already shown evidence suggesting that it is the change in temperature, not surface moisture, that leads to the equatorward contraction of high CAPE values and subsequently precipitation, it is worth examining the changes in surface latent heat flux. The models here employ fixed sea surface temperatures and use the bulk aerodynamic formula to calculate surface evaporation, so they are decoupled from the surface radiation. Therefore, the changes in surface

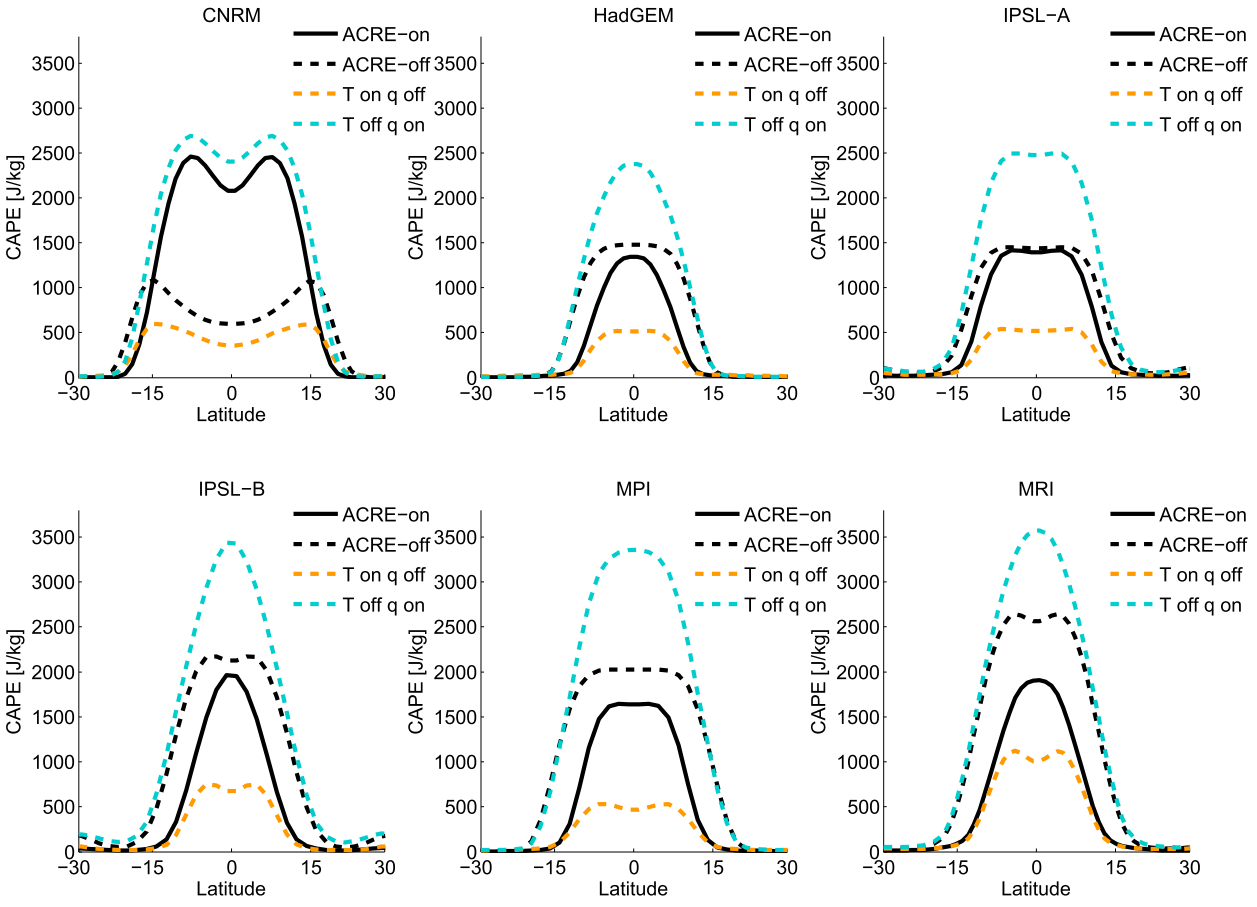


FIG. 5. CAPE for ACRE-on T and q (solid black line), ACRE-off T and q (dashed black line), ACRE-on q and ACRE-off T (dashed teal line), and ACRE-on T and ACRE-off q (dashed orange line) as a function of latitude for all six COOKIE models.

evaporation are driven by changes in the circulation and the need for total precipitation to balance the total atmospheric radiative cooling, not changes in absorbed shortwave at the surface. Despite fixed SSTs and an enhanced mean meridional circulation owing to the cloud radiative heating, the latent heat flux (LHF) does not show a consistent increase from ACRE-off to ACRE-on (Fig. 7). In fact, in three of the models, LHF is consistently weaker for ACRE-on compared to ACRE-off. The other three models have a more complicated meridional structure to their LHF differences. Of course, the increase in horizontal moisture convergence with ACRE is more important for the precipitation, but it is interesting that the latent heat flux fights against that increase. This conflict between moisture convergence and latent heat flux suggests that the zonal winds are slowing down, there is a decrease in eddy-driven gustiness, or there is an increase in boundary layer humidity that can account for the decrease in LHF when the cloud–radiation interactions are included. In short, the LHF often has its greatest decrease right along the equator when the cloud radiative effects are included, which should not encourage convection to move equatorward, and yet that is exactly what is observed. We show later that the mean meridional circulation intensifies with cloud radiative heating included, so the decrease in LHF is more likely due to an increase in low-level humidity (see Fig. 6).

Another possible factor that could influence the upper tropospheric temperature is the boundary layer MSE in the regions of active convection. The increase in moisture convergence near the equator when cloud–radiation interactions are turned on compared to when they are off drives a similar increase in the surface MSE (see Fig. 8). Changes in surface air temperature are small due to the fixed sea surface temperature, and thus it is the moisture convergence driving the magnitude and structure of the surface MSE in the tropics in these models. The increase in surface moisture when cloud–radiation interactions are included supports the idea of enhanced latent heat release in the upper troposphere described above. The increase in boundary layer humidity likely changes the equilibrium of the boundary layer in these models and may introduce additional changes in the low clouds. The low cloud changes may, in turn, feed back on the

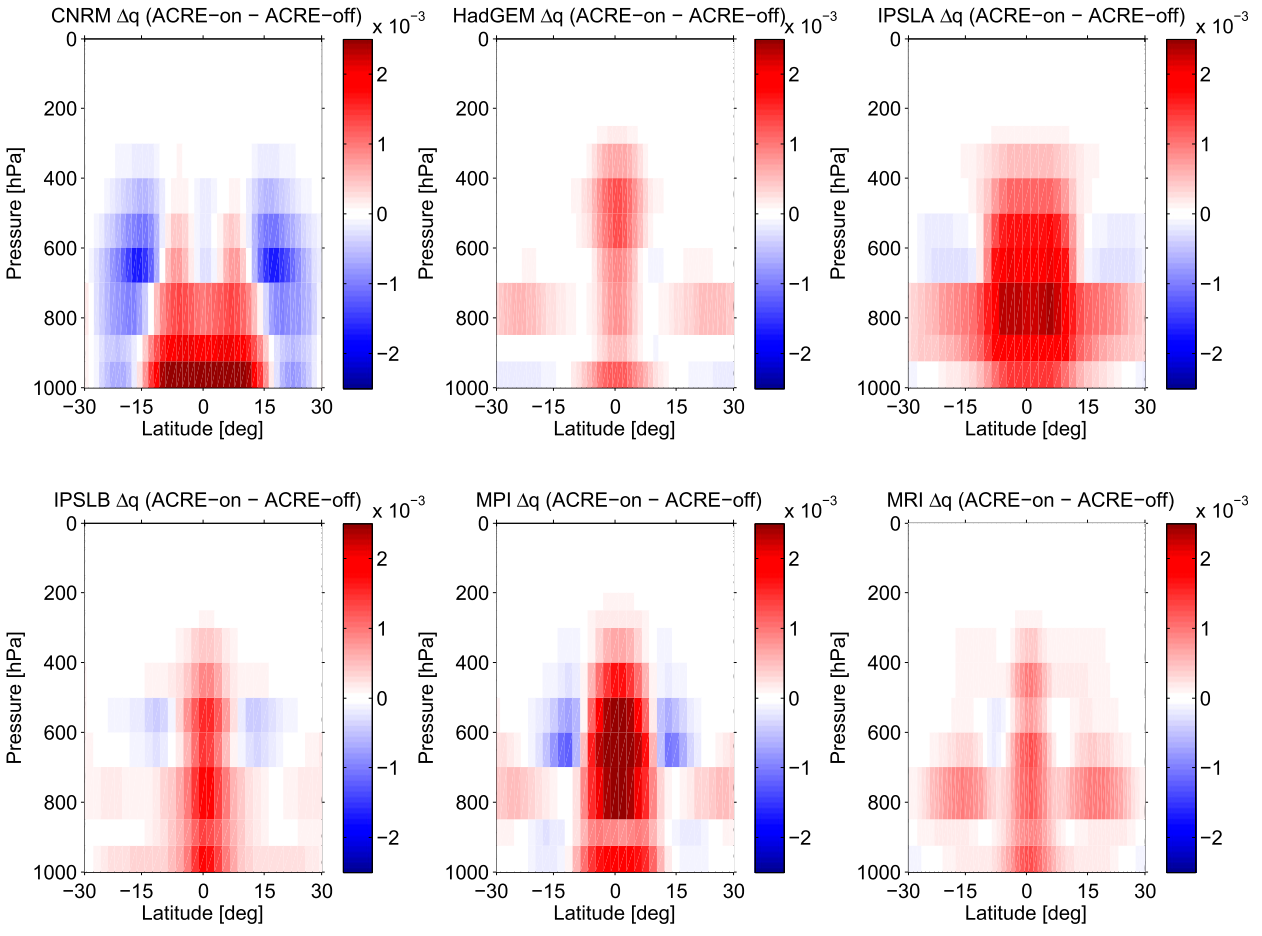


FIG. 6. Specific humidity increase (kg kg^{-1}) caused by the atmospheric cloud radiative effect for all six COOKIE models.

circulation [refer to Fermepin and Bony (2014) for details on the impact of low-cloud ACRE-on circulation changes]. Since the surface air temperature changes little, only the increase in mass flux owing to ACRE is capable of enhancing the vertical sensible heat flux. For most of the models, the difference in surface MSE between ACRE-on and ACRE-off is smaller than the change in upper-tropospheric MSE between ACRE-on and ACRE-off, as expected from the changes in CAPE. The only model that shows a larger change in surface MSE than upper-tropospheric MSE is the CNRM model, which is also the only model that showed an increase in CAPE with ACRE included.

b. *Assessing changes in circulation*

As mentioned above, the change in moisture is primarily the result of circulation changes. ACRE strengthens the mean meridional mass streamfunction in all of the models (see Fig. 9), despite simultaneously increasing the stability. It is expected that the diabatic heating from clouds absorbing longwave radiation has a strong control on the circulation strength, but we want to know whether clear-sky radiatively driven subsidence ω_{rad} (see Kuang and Hartmann 2007; Zelinka and Hartmann 2010; Harrop and Hartmann 2012) may contribute to the increase in circulation strength as well. Radiatively driven subsidence is calculated as follows:

$$\omega_{\text{rad}} = \frac{Q_{\text{rad}}}{\sigma}, \tag{3}$$

where Q_{rad} is the clear-sky radiative cooling, and σ is the static stability. The clear-sky radiative heating terms are not standard output for the COOKIE simulations, thus clear-sky radiative heating was calculated using the RRTMG described for the cloud-resolving model in the section 2. ACRE enhances the clear-sky radiative cooling in the upper troposphere ($p < 500$ hPa), owing to the increase in temperature and moisture at those levels (not shown). ACRE diminishes clear-sky radiative cooling in the midtroposphere ($700 < p < 500$ hPa) for most of the models, owing to the increases in moisture above those levels. ACRE enhances radiatively

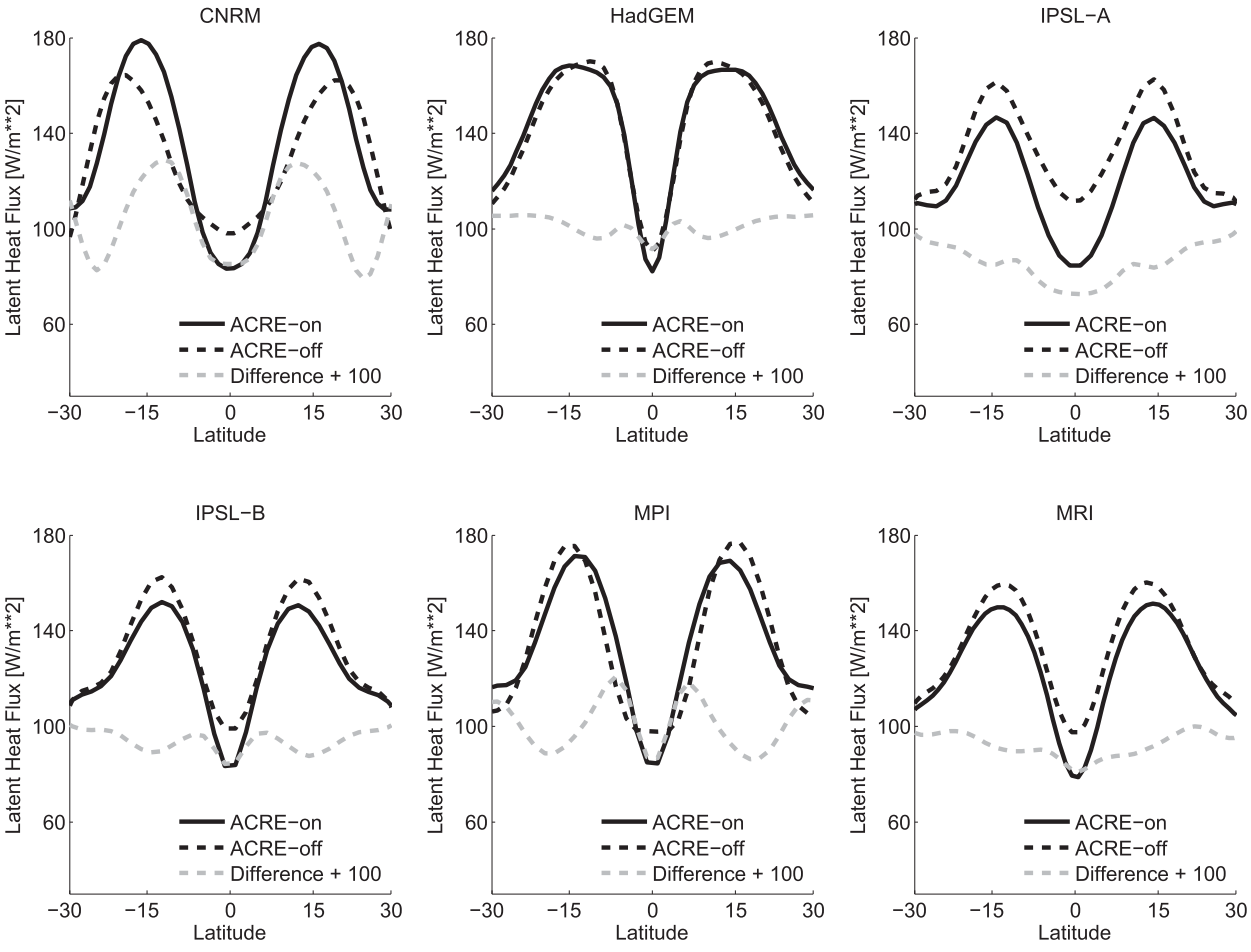


FIG. 7. Latent heat flux for the six different models. The gray dashed line shows the difference ($+100\,\mathrm{W\,m^{-2}}$) between the ACRE-on and ACRE-off experiments.

driven subsidence in the upper troposphere ($100 < p < 300\,\mathrm{hPa}$) but diminishes it in the midtroposphere (see Fig. 10). The enhancement in radiatively driven subsidence is a combination of both changes in the radiative cooling and in the static stability, while the reduction results from the cloud radiative heating increasing static stability compared to when ACRE is removed. The circulation change does not have a strong vertical structure to it, so changes in clear-sky radiative cooling must not drive the circulation response to ACRE. Thus, it is more likely that the direct diabatic heating from convection, not the change in clear-sky radiation, contributes to the change in circulation strength between ACRE-on and ACRE-off.

The distribution of vertical velocities in the COOKIE models depends on the cloud–radiation interactions as well. The probability density functions (PDFs) of vertical velocity at 500 hPa are shown in Fig. 11 for each model. ACRE increases the frequency of strong upward vertical velocities ($\omega_{500} < -100\,\mathrm{hPa\,day^{-1}}$), while also decreasing the frequency of weak upward vertical velocities ($0 < \omega_{500} < -75\,\mathrm{hPa\,day^{-1}}$). Because these are monthly outputs on large grid sizes, the increase in strong upward velocities for ACRE-on could be due to the convective updraft speeds increasing, the frequency of convection within that grid increasing, or a larger area fraction of the grid box being occupied by convection. We will revisit these possibilities later when discussing results from the cloud-resolving model.

The precipitation is enhanced near the equator, but the total precipitation across the tropics (measured as the area between 30°S and 30°N; see Table 2) is less with the cloud radiative effects on owing to the weaker radiative cooling compared to the ACRE-off simulations. Thus, even though the mean circulation is more vigorous with cloud–radiation interactions turned on, there is still less precipitation. The distribution of precipitation, however, is sensitive to the cloud radiative heating and resembles the changes in vertical velocity (see Fig. 12). The ACRE-on simulations have much more frequent heavy precipitation (defined here as rain

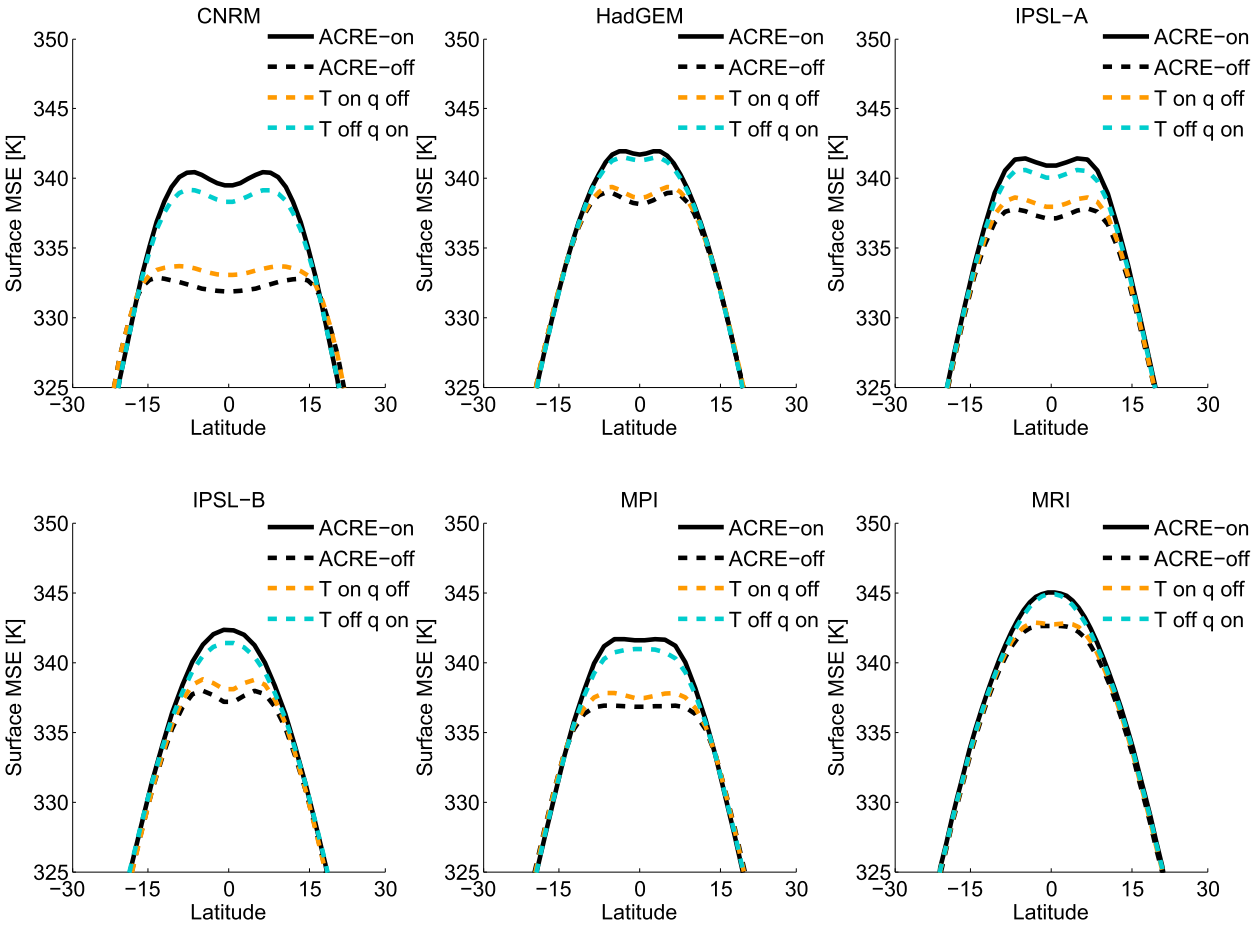


FIG. 8. Surface MSE for the six different models. The black solid line is the ACRE-on simulation while the black dashed line is the ACRE-off simulation. The orange dashed line is the surface MSE calculated using the air temperature from the ACRE-on simulation and the humidity from the ACRE-off simulation. The teal dashed line is the surface MSE calculated using the air temperature from the ACRE-off simulation and the humidity from the ACRE-on simulation. The MPI model did not include surface humidity in the model output database, so we interpolated it using the full 3D humidity field and the surface pressure field.

rates exceeding 20 mm day^{-1}) consistent with the upped-ante mechanism of Neelin et al. (2003) whereby convection is suppressed until the surface MSE is higher.

We suggest that the increase in circulation strength is due to the equator-to-pole atmospheric heating gradient being amplified by ACRE. ACRE is positive in the tropics and negative in the extratropics, requiring greater poleward energy transport (see Figs. 2 and 13). Figure 13 shows the multimodel-mean zonal-mean ACRE, and poleward heat transport for the ACRE-on experiments (left), as well as the difference in these two quantities between ACRE-on and ACRE-off (right). Note that ACRE is zero in the ACRE-off experiments by construction, so ACRE appears the same in both panels of Fig. 13. The poleward energy transport is calculated indirectly using the top-of-atmosphere and surface fluxes, both radiant and turbulent. The poleward energy transport is calculated separately for both ACRE-on and ACRE-off, and thus accounts for changes both in ACRE as well as latent heat flux at the surface. Figure 13 shows that ACRE enhances the poleward energy transport by nearly a petawatt at some latitudes—the integrated increase in poleward energy transport is roughly 15%. Because the sea surface temperatures are held fixed, the surface fluxes do not need to be balanced; thus, the ACRE gradient could be offset by changes in surface fluxes. This does not appear to be the case in these simulations, however, and instead the atmospheric circulation intensifies to transport additional energy poleward. It is likely that since ACRE is primarily driven by longwave heating, in the tropics we would not expect ACRE heating to be taken up by the surface. Therefore, even in a coupled simulation, one might still expect an increase in poleward energy transport by the atmosphere in response to ACRE. Note that there is a strong enhancement of poleward energy transport in the midlatitudes

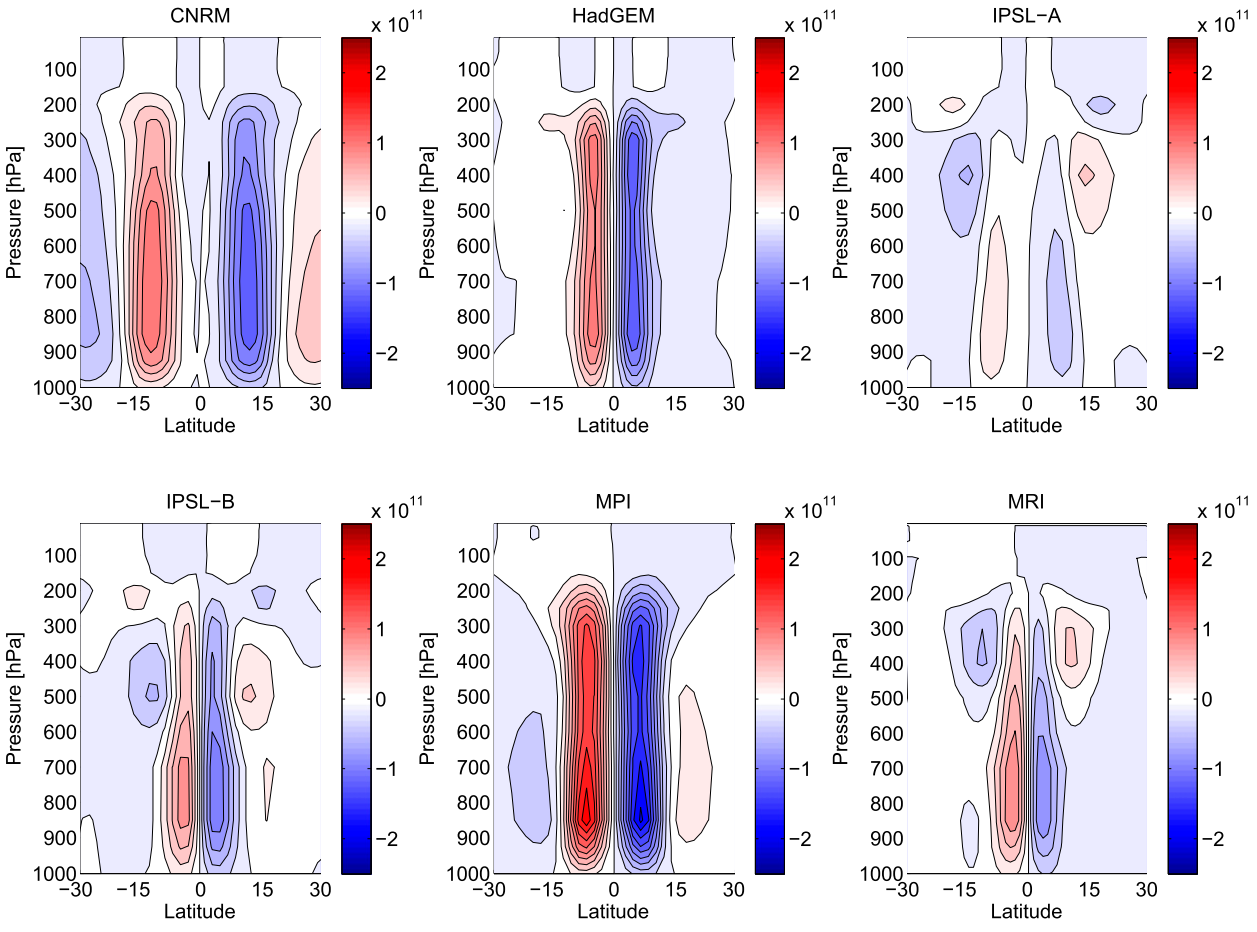


FIG. 9. Difference in mass streamfunction ($kg\,s^{-1}$) between ACRE-on and ACRE-off simulations for all six models. Positive is a counterclockwise circulation anomaly, so that all models show an increase in tropical overturning near the equator in response to cloud radiative forcing.

consistent with an increase in eddy kinetic energy as described by Li et al. (2015).

In the original six models used for COOKIE, we see a consistent increase in integrated cloud water path when the cloud radiative effects are included (see Fig. 14). If we integrate the cloud water path over the tropics (30°S–30°N), we see a consistent increase across the models ranging from 14 to 56 $g\,m^{-2}$. As noted above, over the same region, precipitation decreases when cloud radiative effects are included. A decrease in precipitation with a simultaneous increase in cloud mass would suggest a decrease in precipitation efficiency. Across the tropics, the ratio of precipitation to cloud water path increases from the ACRE-off to the ACRE-on configurations in all models. The decrease in precipitation efficiency occurs even in the deep convective regions.

c. *Investigating a transient experiment*

As noted above, a transient experiment was performed using the GFDL model in aquaplanet mode. We use the Qobs sea surface temperature pattern as before and the SSTs remain fixed throughout the simulation. We have a 2-yr climatology run, followed by an abrupt removal of the cloud radiative effects. The radiative relaxation time of the upper tropical troposphere is on the order of a few weeks (Hartmann et al. 2001), so we expect the transition period from one equilibrium state to the other to occur on a similar time scale. Therefore, we use daily data in the transient experiment to capture the changes. From the hypothesis above, we expect that after the clouds are removed, the temperature in the upper tropical troposphere will begin to decrease while the ITCZ will begin moving poleward. To measure these two impacts, we will use the temperature at 224 hPa (roughly the outflow level for tropical deep convection in the real tropical atmosphere; see Houze and Betts 1981) and the precipitation-weighted latitude. Within the model, substantial detrainment of deep convection (measured by divergence) occurs at the 157-hPa level as well. Our conclusions are not sensitive to the choice of level, so we will

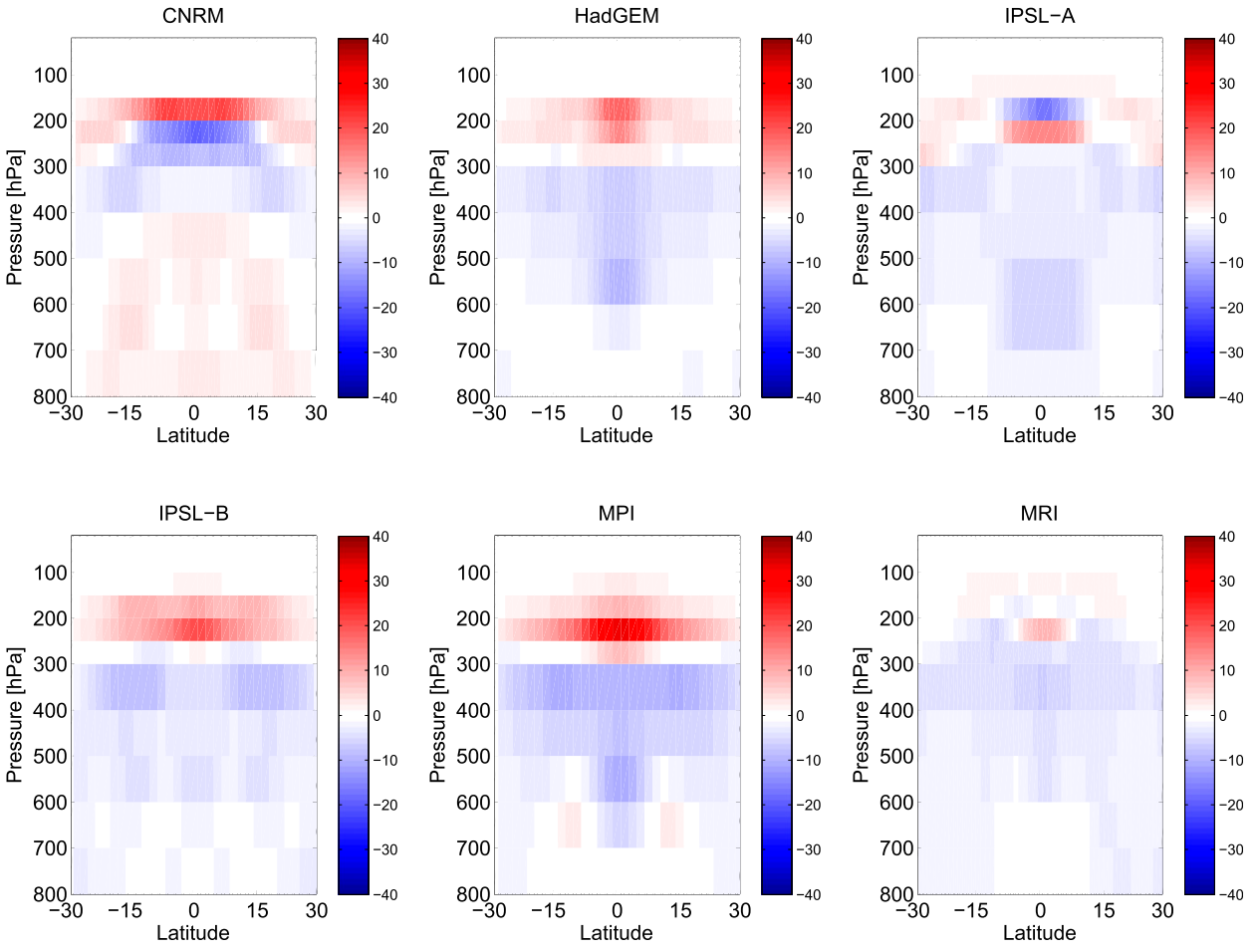


FIG. 10. Difference in radiatively driven subsidence (hPa day^{-1}) above the boundary layer (ACRE-on minus ACRE-off).

focus only on the 224-hPa temperature. We have chosen to average the temperature at 224 hPa over 15°S–15°N. While the magnitude of the temperature change varies across these latitudes, we find that the zonally averaged time rate of change in temperature is the same across 15°S–15°N (not shown). For simplicity, we will refer to the temperature at the 224-hPa pressure level as T_{224}.

Figure 15 shows the time series of T_{224} and ϕ_P during the 100 days before and after the switch from ACRE-on to ACRE-off. We can see from Fig. 15 that the transition from the ACRE-on to the ACRE-off state occurs rapidly. The mean in T_{224} drops from 224 to 222 K. The mean in ϕ_P increases from 7.92° to 9.43° when ACRE is turned off. Despite some low frequency variations in the precipitation signal, we see the simulation reaches its new equilibrium values for T_{224} and ϕ_P within about 40 days. The main conclusion from the transient experiment is that the decrease in upper tropospheric temperature owing to the removal of cloud–radiation interactions accompanies the poleward broadening of the ITCZ, as expected. Note that T_{224} and ϕ_P are significantly correlated over the first 40 days after the cloud radiative effects are removed, but the correlation drops off rapidly after that period such that T_{224} is not a good predictor of the oscillations seen in ϕ_P.

d. *Further testing with a cloud-resolving model*

We have also tested our findings within a cloud-resolving model with two different microphysical configurations (described in section 2). The main difference between the SAM and NA5 microphysics is that the NA5 microphysics produces substantially more high, thin-to-medium optical thickness clouds, in better agreement with satellite observations (Lopez et al. 2009), which exert a greater radiative heating in the atmosphere. As such, the inclusion of the cloud radiative heating increases the domain average atmospheric radiative heating by a lot more in the NA5 configuration than the SAM configuration (7.2 and 0.2 W m^{-2}, respectively). While both of these changes are statistically significant at the 95% level, because the change in radiative heating is so small in the SAM configuration, there is no statistically

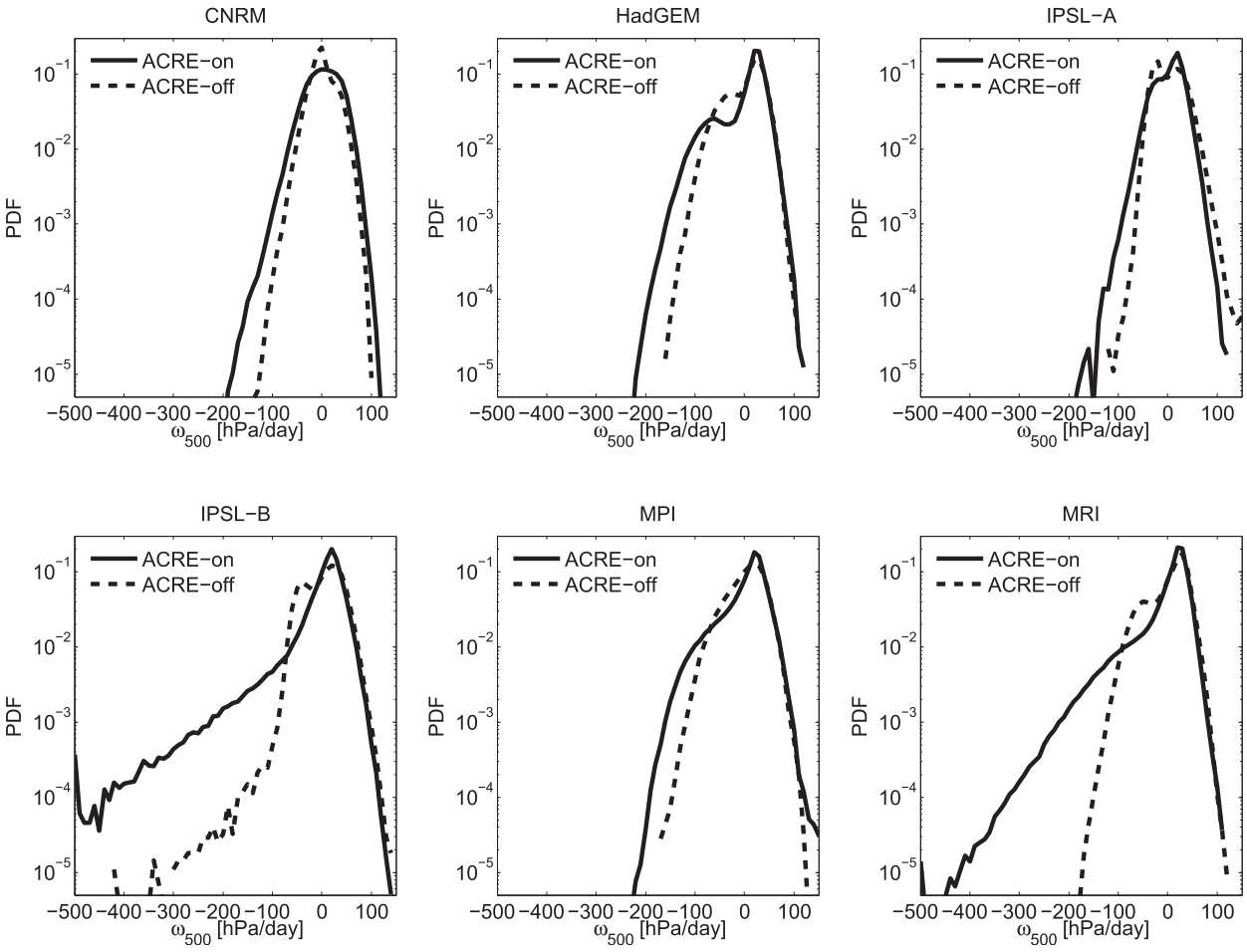


FIG. 11. PDF of 500-hPa vertical velocity for the six different models (30°S–30°N). The solid line is the ACRE-on configuration; the dashed line is the ACRE-off configuration.

significant change in domain-average precipitation for the SAM configuration. The NA5 configuration shows a statistically significant decrease in domain-average precipitation of 0.17 mm day^{-1}. Additionally, Fig. 16 (top) shows that for the NA5 configuration, the spatial extent of precipitation narrows over the warm pool part of the simulation with clouds on, similar to the ITCZ moving closer to the equator in the COOKIE simulations. The response in the SAM configuration is a slight shift of the precipitation without any change in magnitude. It is also worth noting that the mean climate is not the same between the two microphysical configurations in the CRM. The microphysical parameterizations make the temperature higher in the SAM configuration than in the NA5 configuration for ACRE-off. However, the SAM configuration is colder than NA5 for ACRE-on, as expected, owing to stronger cloud radiative heating (not shown). Similar to the COOKIE simulations, the upper tropospheric temperatures are warmer with ACRE-on than ACRE-off for both microphysics configurations in the CRM. The warming in the SAM configuration is smaller than that of NA5, owing to less high cloud in the SAM configuration.

While the mean atmospheric radiative heating changes little between the ACRE-on and ACRE-off simulations in the SAM configuration (see Fig. 16, middle), there is weaker cooling in the convective zones owing to the prevalence of high clouds and stronger cooling in the subsidence zones owing to the prevalence of low clouds there. Thus, the balance between high clouds trapping emissions and low clouds enhancing emissions causes the weak mean response of the radiative heating profile in the SAM configuration. For the NA5 configuration, the high clouds dominate the response, giving the distinct increase in radiative heating in ACRE-on compared to ACRE-off.

The mean vertical velocity at 500 hPa w_{500} in the region of convection is also greater with cloud–radiation interactions present than when they are removed, which agrees with the results from the GCMs. The change in w_{500} between the ACRE-on and ACRE-off simulations

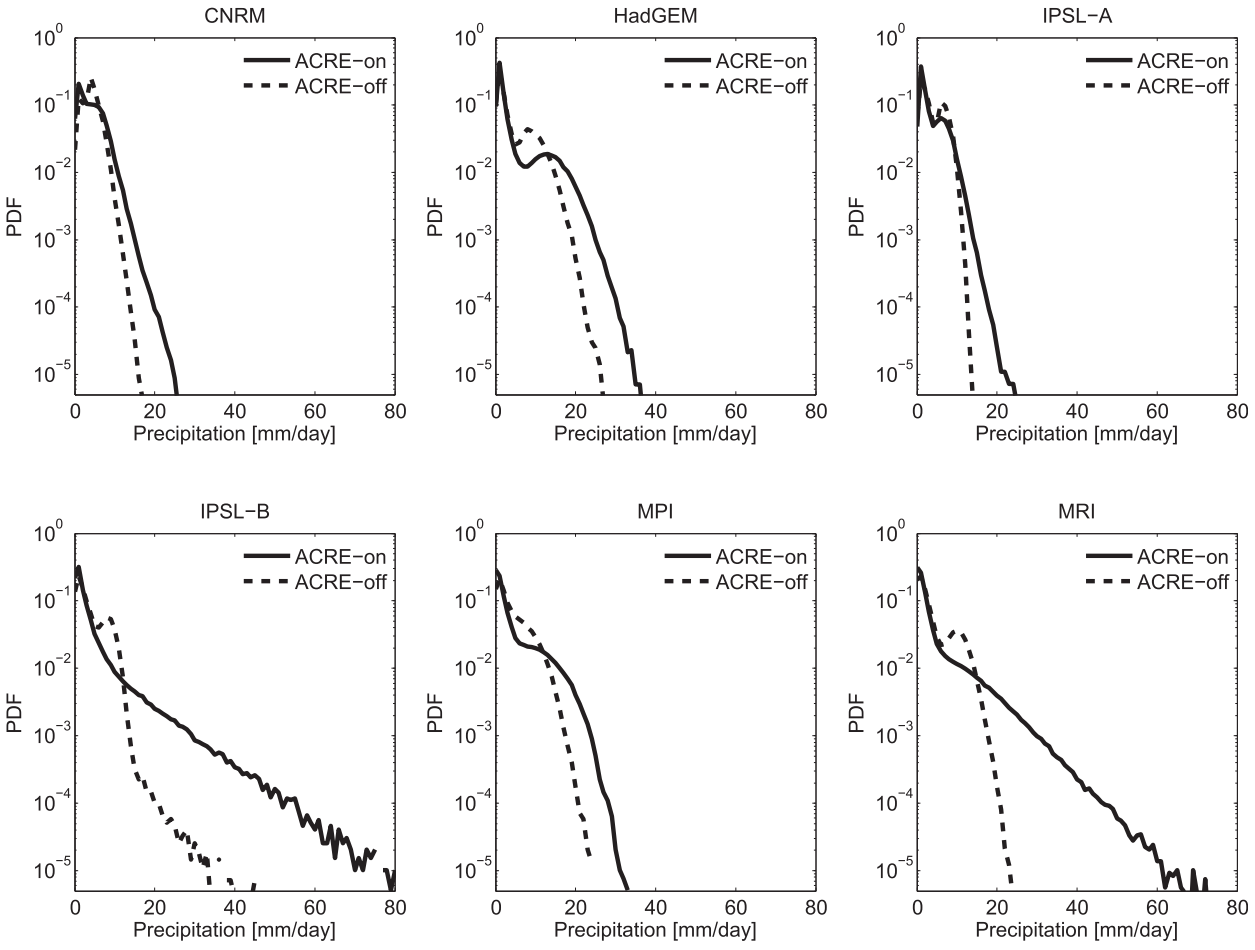


FIG. 12. PDF of precipitation for the six different models (30°S–30°N). The solid line is the ACRE-on configuration; the dashed line is the ACRE-off configuration.

closely resembles the change in precipitation (not shown). Again, as in the GCMs, we see a similar circulation intensification (reflected in the precipitation changes) from ACRE-off to ACRE-on. The heating of the upper atmosphere by clouds stabilizes the atmosphere, but at the same time the gradient in that heating requires the circulation to intensify. The atmosphere responds by contracting precipitation into a narrower, more intense band over the warmest SSTs. The distribution in w_{500} for the CRMs, however, bears little resemblance to the distribution of ω_{500} seen in the GCMs. The difference between the CRM and GCMs is not surprising. The distribution of w_{500} in the CRM shows the frequency of individual updraft speeds, while the distribution of ω_{500} in the GCMs is an aggregation, both in time and space, of numerous updrafts. As an example of this discrepancy, the increase in ω_{500} with ACRE-on for the GCMs could be due to the convective updraft speeds increasing or it could be more frequent updrafts with the same speed as in the ACRE-off configuration. Looking at the CRM, the distribution of w_{500} hardly changes at all between the ACRE-on and ACRE-off configurations for the SAM microphysics, while for the NA5 microphysics, the ACRE-on configuration favors weaker updrafts and downdrafts compared to the ACRE-off configuration (see Fig. 16, bottom). The CRM shows that the vertical velocity of individual convective plumes is not as sensitive to ACRE as the GCMs suggest. If anything, the inclusion of cloud radiative heating weakens the convective updraft speeds.

For both microphysical configurations, the liquid water path (LWP) increases for ACRE-on, while at the same time the ice water path (IWP) decreases. The SAM configuration is roughly 50/50 ratio of liquid and ice, while the NA5 configuration is roughly 25/75 ratio of liquid and ice. The increase in total cloud water path (CWP) in the SAM configuration is small ($+0.77\,\mathrm{g\,m^{-2}}$) owing to the offsetting changes in liquid and ice. In NA5, however, CWP actually decreases ($-9.2\,\mathrm{g\,m^{-2}}$) owing to the relatively stronger influence of ice. In the GCMs,

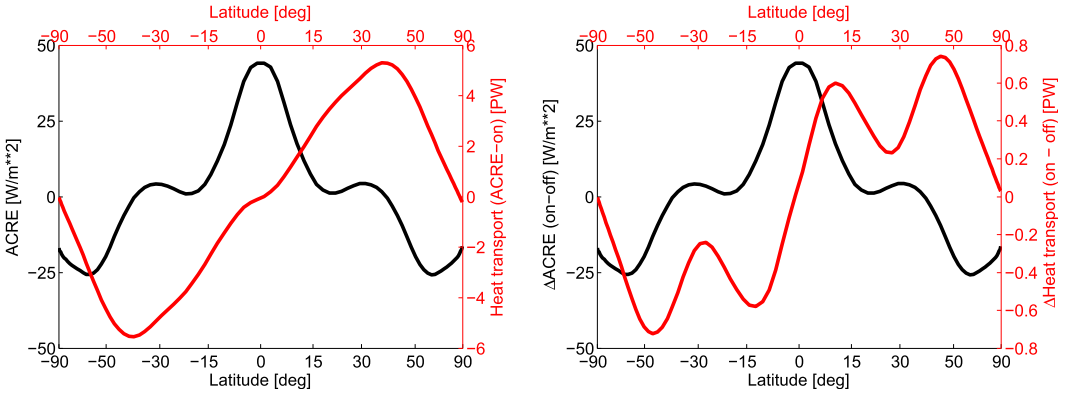


FIG. 13. (left) Multimodel-mean zonal-mean ACRE (black) and atmospheric poleward energy transport (red) for the six COOKIE models. (right) As at (left), but for the difference between ACRE-on and ACRE-off experiments. Note that the poleward energy transport is calculated indirectly from the top-of-atmosphere and surface fluxes, both radiant and turbulent.

both LWP and IWP increase in all models across the tropics (not shown). The increase in LWP is greater than the increase in IWP in all of the GCMs as well.

We performed another set of experiments with the CRM where we used a slab ocean with fixed ocean heat transport in a sinusoidal pattern with amplitude of $25\,\mathrm{W\,m^{-2}}$ and a mean value equal to the top-of-atmosphere radiation imbalance. The model was run into equilibrium with the cloud radiative heating included. We then took those sea surface temperature distributions (one for each microphysics configuration) and ran the ACRE-on and ACRE-off experiments as before. Experiments such as these are useful because they use a natural sea surface temperature distribution—"natural" in the sense that it represents a model-selected climate mode that has the atmosphere and ocean circulations in equilibrium with one another. The resulting changes between the ACRE-on and ACRE-off experiments are similar to those shown above with the fixed sinusoidal SST pattern described in section 2. Therefore, our results from this work with the CRM are robust between the differing SST patterns.

We may expect that the strength of the precipitation contraction may also be sensitive to whether we use 2D or 3D simulations. We have chosen the 2D setup for its simplicity and cost efficiency. While 3D simulations tend to have a different organization pattern for convection compared to 2D simulations, we anticipate that both will produce the vertical heating gradient needed to test our CAPE argument. The magnitude of that heating gradient is likely to change between 2D and 3D experiments, but we do not expect 3D effects to change our basic qualitative conclusions. We have no rotation in our simulations to simplify the problem. Since the CAPE mechanism does not rely on rotation, our results should not be sensitive to whether rotation is included or not.

In short, the cloud-resolving model allows us to investigate whether the conclusions drawn from the COOKIE simulations are sensitive to the GCM framework. While all of the GCMs show a contraction of precipitation over the warmest SSTs when cloud radiative heating is included, the CRM only shows this behavior when high, thin-to-medium optical thickness clouds are prevalent. While the GCMs show a consistent increase in vertical velocity for ACRE-on, the CRM does not. The differences in vertical velocity between the GCMs and the CRM may be sensitive to the inclusion of rotation in the GCMs and the absence of rotation in the CRM. Future research will be needed to assess the combined role of rotation and cloud radiative heating on vertical velocity. In fact, the response of vertical velocities to cloud radiative heating in the CRM depends on which microphysics is used: vertical velocities slow down in NA5, whereas they are insensitive to cloud radiative heating in SAM. We cannot determine whether the GCMs are simply showing the effect of more frequent convection in areas where convection is already prevalent or if they are in disagreement with the CRM. Finally, while the CWP increases robustly in the GCMs, the response of CWP to cloud radiative heating in the CRM shows a strong dependence on microphysics. The main difference between the GCMs and the CRM is in the response of ice water path to cloud radiative heating. The GCMs show IWP increases with cloud radiative heating, while the CRM shows that IWP decreases with cloud radiative heating. Future research will be needed to clarify this difference.

4. Conclusions

In aquaplanet simulations with fixed SSTs, we find that the atmospheric cloud radiative effect (ACRE) results in an equatorward contraction of the ITCZ,

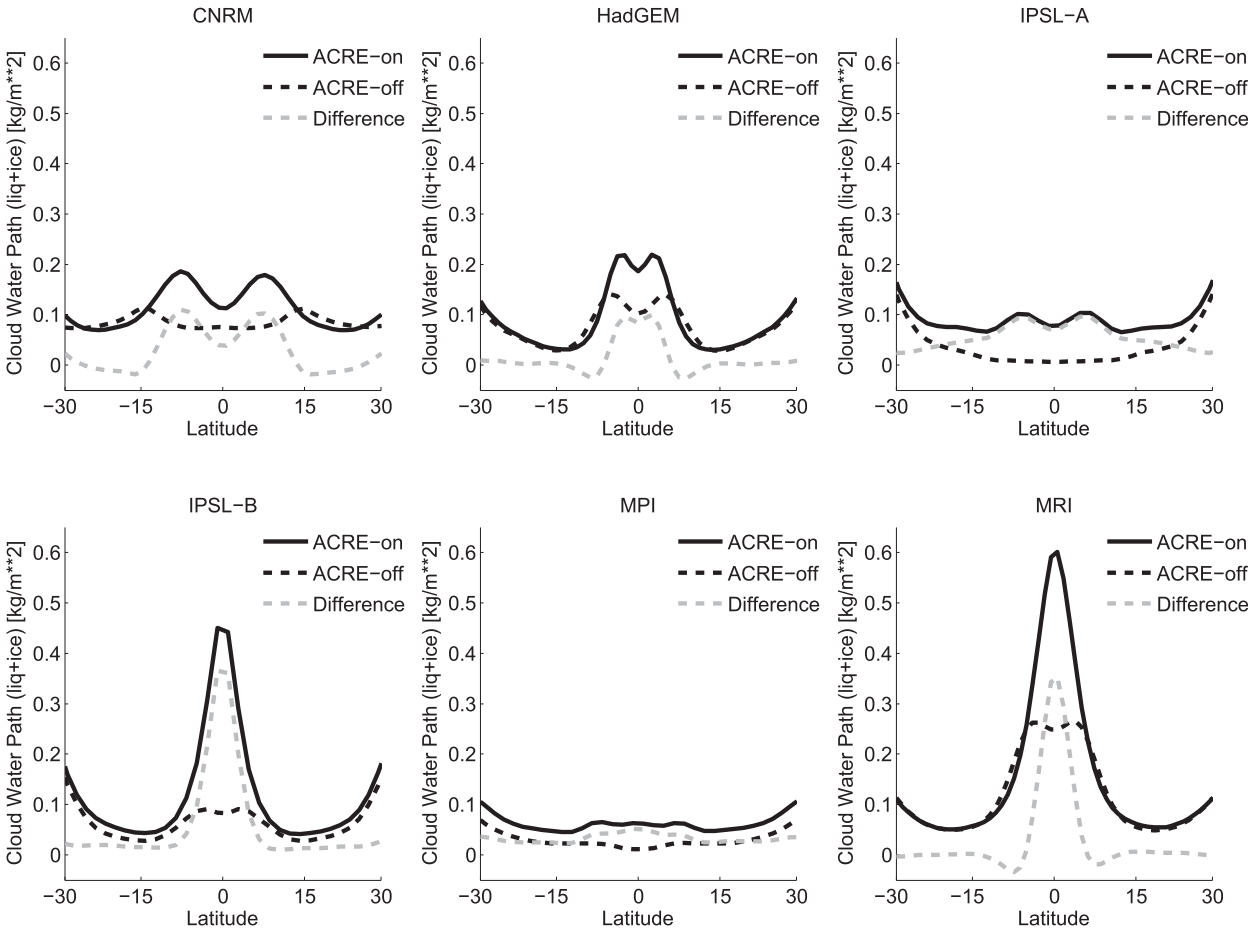


FIG. 14. Cloud water path (liquid + ice) for the six different models. The gray dashed line shows the difference between the ACRE-on and ACRE-off experiments.

and a substantial reduction in the double ITCZ problem in all models. The equatorward contraction in the ITCZ is consistent with the contraction of the tropical CAPE maximum [consistent with the hypothesis of Landu et al. (2014)]. Cloud radiative heating in the tropical upper troposphere increases the temperature there, increasing stability and decreasing CAPE [in agreement with Sherwood et al. (1994)]. While the atmospheric cloud radiative effect is not an effective proxy for how far the ITCZ contracts, the contraction is nonetheless robust across all models despite their differences in resolution, dynamics, and parameterizations. We have also shown that the increase in upper tropospheric temperature from the atmospheric cloud radiative effect smoothly transitions with the ITCZ in a transient simulation from the ACRE-on to the ACRE-off configuration. Our results show a robust ITCZ response across a wide range of model parameters, although none of them consider realistic land–sea geography. The equatorward contraction of the precipitation envelope when including cloud radiative heating agrees with Randall et al. (1989) and with Liu and Moncrieff (2008).

Regarding our use of CAPE (following Landu et al. 2014) as a metric for explaining how the cloud radiative heating forces a contraction of the ITCZ, we note that CAPE is effectively an integrated measure of stability of the atmosphere. Precipitation forms where the atmosphere is most unstable to convection (i.e., where CAPE is highest). While CAPE depends on both temperature and moisture, we have already shown that it is the temperature increase that results in the contraction of the ITCZ in these models. We argue that the cloud radiative heating is responsible for the increase in upper atmospheric temperature. The other major heating term, latent heat release, actually decreases in the tropical average when cloud radiative heating is included owing to a decrease in the radiative cooling of the atmosphere.

Changes in surface turbulent fluxes have been cited in the literature (e.g., Numaguti 1993; Barsugli et al. 2005;

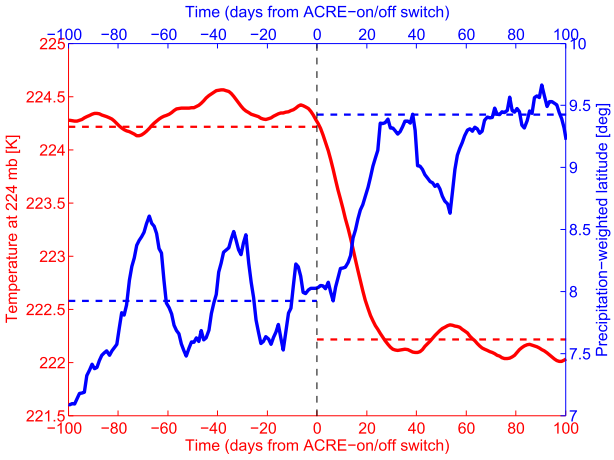


FIG. 15. Time series of temperature at 224 hPa averaged over 15°S–15°N (red) and of ϕ_P (blue). Day 0 is the transition from radiatively active to radiatively inactive clouds. The data are smoothed by a boxcar smoother of 15 days. The horizontal dashed lines represent the mean values of the equilibrated simulation prior to and after the transition. Data are taken from the GFDL transient simulation run for this study.

Möbis and Stevens 2012; Liu et al. 2010) as a cause for a change from single to double ITCZ within models. Our results suggest a change in latent heat flux is not responsible for the equatorward contraction of the ITCZ due to ACRE. In fact, in some of the models, the strongest decrease in LHF occurs on the equator, which would not be expected to draw the ITCZ equatorward. Evaporation changes are likely still important for determining the climatology of the ACRE-on simulations, and may even contribute to the magnitude of the equatorward contraction of the ITCZ when cloud–radiation interactions are included, but they are not responsible for the robust ITCZ contractions seen here. Changes in surface turbulent fluxes do offset changes in atmospheric radiative heating, as expected.

The models further show a robust increase in precipitation in convective regions in the ACRE-on compared to ACRE-off configurations, confirming results from prior studies (e.g., Slingo and Slingo 1988, 1991; Randall et al. 1989). Across the whole of the tropics, however, the total precipitation decreases to balance the reduction in radiative cooling when the cloud–radiation interactions are present. The cloud radiative effects enhance the mean meridional circulation in all models, again confirming prior studies (e.g., Ramanathan 1987; Slingo and Slingo 1988, 1991; Stuhlmann and Smith 1988a,b; Randall et al. 1989; Sherwood et al. 1994; Zhang and Rossow 1997; Sohn 1999; Bergman and Hendon 2000a,b; Raymond 2000; Tian et al. 2001; Tian and Ramanathan 2002, 2003; Lee and Yoo 2014; Del Genio and Chen 2015; Crueger and Stevens 2015). Tian and Ramanathan (2003) showed that a realistic ACRE distribution can recreate quantitatively realistic Hadley and Walker circulations. Also, we have shown that the clear-sky radiative cooling cannot be responsible for the circulation increase. We therefore suggest that it is the enhanced meridional gradient in diabatic heating caused by ACRE (heating in the tropics and cooling in the extratropics) that is responsible for the circulation intensification. Despite the decrease in precipitation and increase in stability in the tropics, the enhanced energy flux poleward requires the circulation to speed up. Further research into this area needs to be done to see how robust this mechanism is.

The clouds also act to partition more of the net divergence of energy transport into the atmosphere instead of the ocean (Zhang and Rossow 1997; Tian et al. 2001). Removing cloud radiative heating while keeping SSTs fixed increases the implied zonally averaged values of ocean heat transport up above 100 $\mathrm{W\,m^{-2}}$ along the equator (depending on the model), which is more characteristic of the cold tongue than the actual tropical mean in the real world. While fixed SSTs are a useful experiment for isolating the impact of the cloud radiative heating on the circulation, it is worth noting that the total climate response to removing cloud–radiation interactions would change in coupled atmosphere–ocean models, particularly since we expect the shortwave effect of clouds to have a strong influence on SST.

Not only does cloud radiative heating reduce tropics-wide precipitation, it also changes the distribution of precipitation intensities to favor heavier precipitation (rates exceeding 20 $\mathrm{mm\,day^{-1}}$). Additionally, we have quantified the changes in the vertical velocity distribution across the various GCMs as well as within a pair of cloud-resolving model simulations. The GCMs show a robust increase in both stronger precipitation rates and updraft speeds when cloud radiative heating is included. The CRM simulations, however, suggest that the frequency of strong updraft speeds does not actually increase in response to cloud radiative heating. Of course, a Hadley cell on a spherical Earth is different from the 2D nonrotating circulation in the CRM, so the geometry and rotation of the GCMs may factor into the differences in vertical velocity as well. Future research should look to determine whether the absorption of radiation by clouds is capable of enhancing the updraft speed within individual convective storms.

Cloud radiative heating and its subsequent enhancement of the circulation increase column-integrated cloud liquid and ice mass [the cloud water path (CWP)]. The decrease in precipitation and increase in cloud mass suggests that cloud radiative effects reduce precipitation efficiency, meaning that more high clouds are generated

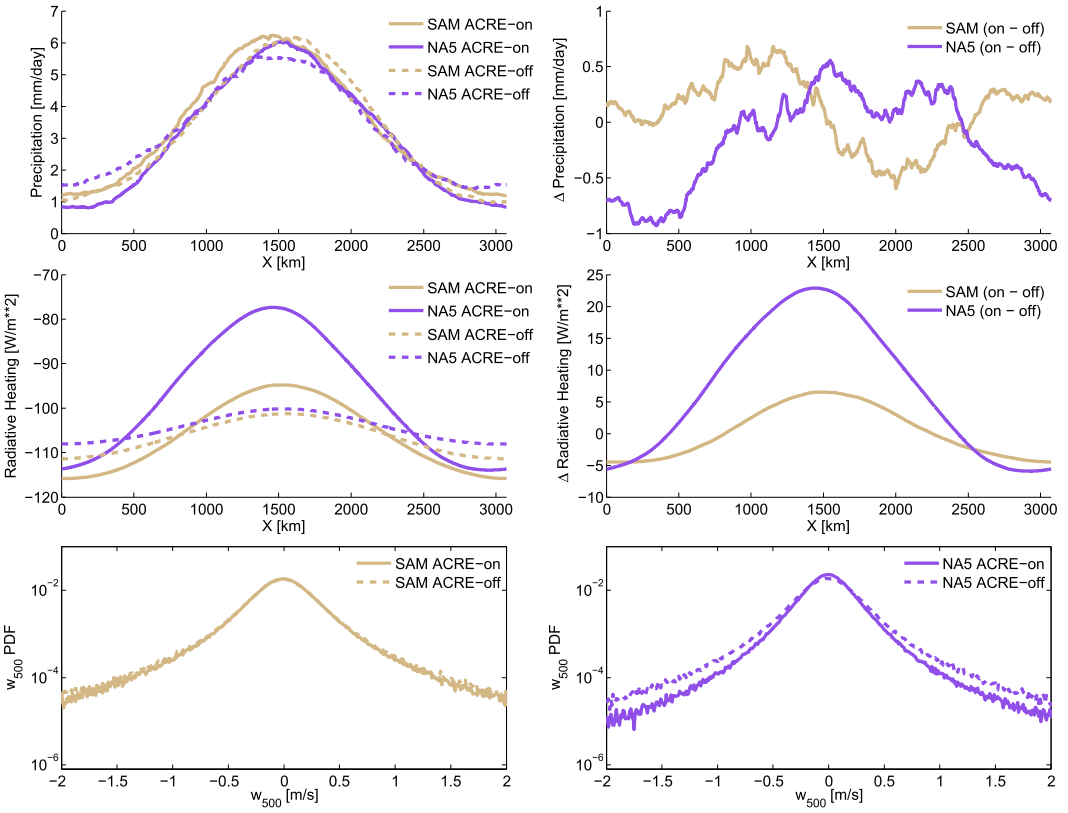


FIG. 16. (top left) mean precipitation amounts for both microphysics settings (SAM in gold and NA5 in purple) and for both cloud–radiation configurations (ACRE-on and ACRE-off); (top right) difference (ACRE-on minus ACRE-off) in precipitation. (middle left) Mean radiative heating rate for both microphysics (SAM and NA5) and both cloud–radiation configurations (ACRE-on and ACRE-off); (middle right) differences (ACRE-on minus ACRE-off) in cloud water path. (bottom left) PDFs of vertical velocity at 500 hPa for both cloud–radiation configurations with the SAM microphysics; (bottom right) as at (bottom left), but for the NA5 microphysics.

per unit of precipitation, including regions of deep convection. Both the liquid and ice increase across the tropics in all of the GCMs, with liquid increases being the larger component of the CWP increase. In the CRM simulations, however, only liquid water path increases in the presence of cloud radiative heating. The ice water path, shows a decrease from the ACRE-off to ACRE-on configuration in the CRM. The total change in cloud water path is sensitive to the relative abundance of liquid and ice in the mean climate, which is sensitive to the microphysical parameters. Future research should investigate the response of ice abundance to cloud radiative heating.

It is worth taking a moment to elaborate on the differences between our results and those of a few similar studies that had contrasting results. First, Raymond (2000) used a simple beta plane model with parameterized cumulus convection and he found that precipitation maximized over the warmest SSTs with and without cloud–radiation interactions included. The way he defines whether deep or shallow convection occurs is based on whether surface equivalent potential temperature exceeds some threshold. That threshold is defined as the interpolated value of saturated equivalent potential temperature taken where a surface lifted parcel has a total water mixing ratio (vapor + cloud condensate) equal to 1.1 times the saturation mixing ratio. Thus, deep convection may be overly sensitive to surface moisture.

Second, Chao and Chen (2004) used aquaplanet models with experiments both including and removing cloud–radiation interactions. Chao and Chen (2004) show that the position of the ITCZ within their model is not sensitive to whether the cloud–radiation interactions are active in their model, while our analyses show a robust equatorward movement of the ITCZ when cloud–radiation interactions are included. The difference is likely in the sea surface temperature profiles. While the COOKIE simulations all use the Qobs sea surface temperature profile outlined in the Aqua-Planet Experiment project, Chao and Chen (2004) use a globally uniform sea surface temperature. We suspect that the simulations performed by Chao and Chen (2004) show a similar increase in upper tropospheric temperature

when the cloud–radiation interactions are included. However, since the sea surface temperature has no gradient, there would be no equatorward contraction of the high CAPE region; instead CAPE would simply decrease where it was high before.

Third, Wofsy and Kuang (2012) used a cloud-resolving model to investigate the relationship between the precipitation area and radiative cooling and found that increased radiative cooling led to a narrowing of the precipitating region. In our results, the decrease in radiative cooling owing to the tropical clouds constrains the precipitation region to be closer to the equator, effectively narrowing it. The radiative cooling in the Wofsy and Kuang (2012) study was a fixed value throughout the depth of the troposphere, however, so the CAPE-driven arguments resulting from the vertical distribution of cloud heating would not apply to their study.

Finally, Voigt and Shaw (2015) showed that changes in ACRE with global warming caused precipitation to contract in one aquaplanet model but expand in a different model, suggesting that the role of ACRE with regard to the meridional distribution of precipitation depends on the climate state. In their results, they break down the components of the precipitation changes into those driven by SST, ACRE, and water vapor radiative heating. They show that increasing SST increases precipitation everywhere in the tropics, but the increases are largest right along the equator, similar to a contraction of the ITCZ. The same can be seen in the vertical velocity field (see Fig. 2f in Voigt and Shaw 2015); upward vertical velocities are enhanced right along the equator and decrease just off the equator. Because the temperature profile of the tropical atmosphere above the boundary layer is nearly moist adiabatic, the upper atmosphere warms more than the surface, creating a vertical temperature gradient similar to that caused by ACRE. Therefore, in the case of their increasing SST experiments, their results are in line with our own. The response of precipitation to ACRE in the simulations examined by Voigt and Shaw (2015) is not a result of the climatological ACRE profile but rather from the changes in meridional ACRE distribution brought about by warming. It is reasonable to expect that cloud feedbacks may not reflect a simple amplification of the climatological cloud patterns. While the model physics have all been developed to give reasonable mean climate states (in AMIP- or CMIP-type experiments, at least), their feedbacks are not nearly as well constrained. It is unclear whether the stability changes from the cloud feedbacks are the same between the two models examined by Voigt and Shaw (2015). Based on the results found here, it is likely that they are not. This same rationale applies to the circulation strength as well; cloud feedbacks that differ between models are also likely to differ on the response of the Hadley circulation to warming.

As this work and previous work have shown, there are many processes important for determining the climatological mean position of the ITCZ. This work emphasizes the role of local cloud radiative heating processes in constraining the ITCZ to the regions of maximum SST. Precipitation hews more closely to the maximum SST locations when cloud radiative effects are included. It is important to note that all of these simulations have been conducted with fixed SSTs, and more complicated feedback processes involving changes in the SST patterns may exist in coupled simulations. These results further highlight the importance of getting the cloud–radiation interactions correct in models—the amount of heating that occurs not only at the top of the atmosphere but also within the atmosphere is of critical importance for the location and strength of precipitation and for atmospheric circulation.

Follow-up research will look at cloud macrophysical responses (cloud area, cloud-top temperature, etc.) to cloud radiative heating. Additional research will look into whether these effects are amplified or diminished in a warmer or CO_2-rich environment. The enhanced CO_2, for example, may reduce the amount of longwave absorbed by the clouds and limit ACRE. GCMs also tend to have a reduction in high cloud fraction at warmer temperatures, which would also reduce ACRE.

Acknowledgments. We acknowledge the World Climate Research Programme's Working Group on Coupled Modelling, which is responsible for CMIP, and we thank the climate modeling groups (listed in Table 1 of this paper) for producing and making available their model output. For CMIP the U.S. Department of Energy's Program for Climate Model Diagnosis and Intercomparison provides coordinating support and led development of software infrastructure in partnership with the Global Organization for Earth System Science Portals. The authors thank Paulo Ceppi for his help running the GFDL AM2.1 model. The authors also would like to thank George Bryan for access to his script to calculate CAPE. The authors would also like to thank all of the reviewers for their helpful comments in revising this manuscript. Funding for this work was provided by NSF Grant AGS-0960497.

REFERENCES

Anderson, J., and Coauthors, 2004: The New GFDL Global Atmosphere and Land Model AM2–LM2: Evaluation with prescribed SST simulations. *J. Climate*, 4641–4673, doi:10.1175/JCLI-3223.1.

Arakawa, A., and W. H. Schubert, 1974: Interaction of a cumulus cloud ensemble with the large-scale environment, Part I.

J. Atmos. Sci., **31**, 674–701, doi:10.1175/1520-0469(1974)031<0674:IOACCE>2.0.CO;2.

Barsugli, J., S.-I. Shin, and P. D. Sardeshmukh, 2005: Tropical climate regimes and global climate sensitivity in a simple setting. *J. Atmos. Sci.*, **62**, 1226–1240, doi:10.1175/JAS3404.1.

Bergman, J. W., and H. H. Hendon, 2000a: Cloud radiative forcing of the low-latitude tropospheric circulation: Linear calculations. *J. Atmos. Sci.*, **57**, 2225–2245, doi:10.1175/1520-0469(2000)057<2225:CRFOTL>2.0.CO;2.

——, and ——, 2000b: The impact of clouds on the seasonal cycle of radiative heating over the Pacific. *J. Atmos. Sci.*, **57**, 545–566, doi:10.1175/1520-0469(2000)057<0545:TIOCOT>2.0.CO;2.

Bryan, G. H., and J. M. Fritsch, 2004: A reevaluation of ice-liquid water potential temperature. *Mon. Wea. Rev.*, **132**, 2421–2431, doi:10.1175/1520-0493(2004)132<2421:AROIWP>2.0.CO;2.

Chao, W. C., and B. Chen, 2004: Single and double ITCZ in an aqua-planet model with constant sea surface temperature and solar angle. *Climate Dyn.*, **22**, 447–459, doi:10.1007/s00382-003-0387-4.

Collins, W., and Coauthors, 2008: Evaluation of HadGEM2 model. Met Office Hadley Centre Tech. Note 74, 47 pp.

Crueger, T., and B. Stevens, 2015: The effect of atmospheric radiative heating by clouds on the Madden–Julian oscillation. *J. Adv. Model. Earth Syst.*, **7**, 854–864, doi:10.1002/2015MS000434.

Dahms, E., H. Borth, F. Lunkeit, and K. Fraedrich, 2011: ITCZ splitting and the influence of large-scale eddy fields on the tropical mean state. *J. Meteor. Soc. Japan*, **89**, 399–411, doi:10.2151/jmsj.2011-501.

Del Genio, A. D., and Y. Chen, 2015: Cloud-radiative driving of the Madden–Julian oscillation as seen by the A-Train. *J. Geophys. Res. Atmos.*, **120**, 5344–5356, doi:10.1002/2015JD023278.

Dufresne, J. L., and Coauthors, 2013: Climate change projections using the IPSL-CM5 Earth System Model: From CMIP3 to CMIP5. *Climate Dyn.*, **40**, 2123–2165, doi:10.1007/s00382-012-1636-1.

Fermepin, S., and S. Bony, 2014: Influence of low-cloud radiative effects on tropical circulation and precipitation. *J. Adv. Model. Earth Syst.*, **6**, 513–526, doi:10.1002/2013MS000288.

Flato, G., and Coauthors, 2013: Evaluation of climate models. *Climate Change 2013: The Physical Science Basis*, T. F. Stocker et al., Eds., Cambridge University Press, 741–866, doi:10.1017/CBO9781107415324.020.

Harrop, B. E., and D. L. Hartmann, 2012: Testing the role of radiation in determining tropical cloud-top temperature. *J. Climate*, **25**, 5731–5747, doi:10.1175/JCLI-D-11-00445.1.

——, and ——, 2015: The relationship between atmospheric convective radiative effect and net energy transport in the tropical warm pool. *J. Climate*, **28**, 8620–8633, doi:10.1175/JCLI-D-15-0151.1.

Hartmann, D. L., 1994: *Global Physical Climatology*. Academic Press, 411 pp.

——, J. R. Holton, and Q. Fu, 2001: The heat balance of the tropical tropopause, cirrus, and stratospheric dehydration. *Geophys. Res. Lett.*, **28**, 1969–1972, doi:10.1029/2000GL012833.

Hoskins, B., R. Neale, M. Rodwell, and G.-Y. Yang, 1999: Aspects of the large-scale tropical atmospheric circulation. *Tellus*, **51B**, 33–44, doi:10.1034/j.1600-0889.1999.00004.x.

Hourdin, F., and Coauthors, 2013a: Impact of the LMDZ atmospheric grid configuration on the climate and sensitivity of the IPSL-CM5A coupled model. *Climate Dyn.*, **40**, 2167–2192, doi:10.1007/s00382-012-1411-3.

——, and Coauthors, 2013b: LMDZ5B: The atmospheric component of the IPSL climate model with revisited parameterizations for clouds and convection. *Climate Dyn.*, **40**, 2193–2222, doi:10.1007/s00382-012-1343-y.

Houze, R. A., and A. K. Betts, 1981: Convection in GATE. *Rev. Geophys.*, **19**, 541–576, doi:10.1029/RG019i004p00541.

Hubert, L. F., A. F. Krueger, and J. S. Winston, 1969: The double intertropical convergence zone—Fact or fiction? *J. Atmos. Sci.*, **26**, 771–773, doi:10.1175/1520-0469(1969)026<0771:TDICZF>2.0.CO;2.

Iacono, M. J., J. S. Delamere, E. J. Mlawer, M. W. Shephard, S. A. Clough, and W. D. Collins, 2008: Radiative forcing by long-lived greenhouse gases: Calculations with the AER radiative transfer models. *J. Geophys. Res.*, **113**, D13103, doi:10.1029/2008JD009944.

Khairoutdinov, M. F., and D. A. Randall, 2003: Cloud resolving modeling of the ARM summer 1997 IOP: Model formulation, results, uncertainties, and sensitivities. *J. Atmos. Sci.*, **60**, 607–625, doi:10.1175/1520-0469(2003)060<0607:CRMOTA>2.0.CO;2.

Kuang, Z., and D. L. Hartmann, 2007: Testing the fixed anvil temperature hypothesis in a cloud-resolving model. *J. Climate*, **20**, 2051–2057, doi:10.1175/JCLI4124.1.

Landu, K., L. R. Leung, S. Hagos, V. Vinoj, S. A. Rauscher, T. Ringler, and M. Taylor, 2014: The dependence of ITCZ structure on model resolution and dynamical core in aqua-planet simulations. *J. Climate*, **27**, 2375–2385, doi:10.1175/JCLI-D-13-00269.1.

Lee, S., and C. Yoo, 2014: On the causal relationship between poleward heat flux and the equator-to-pole temperature gradient: A cautionary tale. *J. Climate*, **27**, 6519–6525, doi:10.1175/JCLI-D-14-00236.1.

Li, G., and S. P. Xie, 2014: Tropical biases in CMIP5 multimodel ensemble: The excessive equatorial Pacific cold tongue and double ITCZ problems. *J. Climate*, **27**, 1765–1780, doi:10.1175/JCLI-D-13-00337.1.

Li, Y., D. W. J. Thompson, and S. Bony, 2015: The influence of atmospheric cloud radiative effects on the large-scale atmospheric circulation. *J. Climate*, **28**, 7263–7278, doi:10.1175/JCLI-D-14-00825.1.

Lin, J.-L., 2007: The double-ITCZ problem in IPCC AR4 coupled GCMs: Ocean–atmosphere feedback analysis. *J. Climate*, **20**, 4497–4525, doi:10.1175/JCLI4272.1.

Liu, C., and M. W. Moncrieff, 2008: Explicitly simulated tropical convection over idealized warm pools. *J. Geophys. Res.*, **113**, D21121, doi:10.1029/2008JD010206.

Liu, Y., L. Guo, G. Wu, and Z. Wang, 2010: Sensitivity of ITCZ configuration to cumulus convective parameterizations on an aqua planet. *Climate Dyn.*, **34**, 223–240, doi:10.1007/s00382-009-0652-2.

Lopez, M. A., D. L. Hartmann, P. N. Blossey, R. Wood, C. S. Bretherton, and T. L. Kubar, 2009: A test of the simulation of tropical convective cloudiness by a cloud-resolving model. *J. Climate*, **22**, 2834–2849, doi:10.1175/2008JCLI2272.1.

Lorenz, E. N., 1967: The nature and theory of the general circulation of the atmosphere. *WMO Bull.*, **16**, 74–78.

Mechoso, C., and Coauthors, 1995: The seasonal cycle over the tropical Pacific in coupled ocean–atmosphere general circulation models. *Mon. Wea. Rev.*, **123**, 2825–2838, doi:10.1175/1520-0493(1995)123<2825:TSCOTT>2.0.CO;2.

Medeiros, B., B. Stevens, I. M. Held, M. Zhao, D. L. Williamson, J. G. Olson, and C. S. Bretherton, 2008: Aquaplanets, climate sensitivity, and low clouds. *J. Climate*, **21**, 4974–4991, doi:10.1175/2008JCLI1995.1.

——, ——, and S. Bony, 2015: Using aquaplanets to understand the robust responses of comprehensive climate models to forcing. *Climate Dyn.*, **44**, 1957–1977, doi:10.1007/s00382-014-2138-0.

Merlis, T. M., 2015: Direct weakening of tropical circulations from masked CO_2 radiative forcing. *Proc. Natl. Acad. Sci. USA*, **112**, 13 167–13 171, doi:10.1073/pnas.1508268112.

Miura, H., H. Tomita, T. Nasuno, S. I. Iga, M. Satoh, and T. Matsuno, 2005: A climate sensitivity test using a global cloud resolving model under an aqua planet condition. *Geophys. Res. Lett.*, **32**, L19717, doi:10.1029/2005GL023672.

Mlawer, E. J., S. J. Taubman, P. D. Brown, M. J. Iacono, and S. A. Clough, 1997: Radiative transfer for inhomogeneous atmospheres: RRTM, a validated correlated-k model for the longwave. *J. Geophys. Res.*, **102**, 16 663–16 682, doi:10.1029/97JD00237.

Möbis, B., and B. Stevens, 2012: Factors controlling the position of the intertropical convergence zone on an aquaplanet. *J. Adv. Model. Earth Syst.*, **4**, M00A04, doi:10.1029/2012MS000199.

Neale, R. B., and B. J. Hoskins, 2000: A standard test for AGCMs including their physical parametrizations: I: The proposal. *Atmos. Sci. Lett.*, **1**, 101–107, doi:10.1006/asle.2000.0022.

Neelin, J. D., C. Chou, and H. Su, 2003: Tropical drought regions in global warming and El Niño teleconnections. *Geophys. Res. Lett.*, **30**, 2275, doi:10.1029/2003GL018625.

Numaguti, A., 1993: Dynamics and energy balance of the Hadley circulation and the tropical precipitation zones: Significance of the distribution of evaporation. *J. Atmos. Sci.*, **50**, 1874–1887, doi:10.1175/1520-0469(1993)050<1874:DAEBOT>2.0.CO;2.

Oueslati, B., and G. Bellon, 2013a: Convective entrainment and large-scale organization of tropical precipitation: Sensitivity of the CNRM-CM5 hierarchy of models. *J. Climate*, **26**, 2931–2946, doi:10.1175/JCLI-D-12-00314.1.

——, and ——, 2013b: Tropical precipitation regimes and mechanisms of regime transitions: Contrasting two aquaplanet general circulation models. *Climate Dyn.*, **40**, 2345–2358, doi:10.1007/s00382-012-1344-x.

Ramanathan, V., 1987: The role of Earth radiation budget studies in climate and general circulation research. *J. Geophys. Res.*, **92**, 4075–4095, doi:10.1029/JD092iD04p04075.

Randall, D. A., D. A. Dazlich, and T. G. Corsetti, 1989: Interactions among radiation, convection, and large-scale dynamics in a general circulation model. *J. Atmos. Sci.*, **46**, 1943–1970, doi:10.1175/1520-0469(1989)046<1943:IARCAL>2.0.CO;2.

Raymond, D. J., 2000: The Hadley circulation as a radiative–convective instability. *J. Atmos. Sci.*, **57**, 1286–1297, doi:10.1175/1520-0469(2000)057<1286:THCAAR>2.0.CO;2.

Sherwood, S. C., V. Ramanathan, T. P. Barnett, M. K. Tyree, and E. Roeckner, 1994: Response of an atmospheric general circulation model to radiative forcing of tropical clouds. *J. Geophys. Res.*, **99**, 20 829–20 845, doi:10.1029/94JD01632.

Slingo, A., and J. M. Slingo, 1988: The response of a general circulation model to cloud longwave radiative forcing. I: Introduction and initial experiments. *Quart. J. Roy. Meteor. Soc.*, **114**, 1027–1062, doi:10.1002/qj.49711448209.

Slingo, J. M., and A. Slingo, 1991: The response of a general circulation model to cloud longwave radiative forcing. II: Further studies. *Quart. J. Roy. Meteor. Soc.*, **117**, 333–364, doi:10.1002/qj.49711749805.

Sohn, B.-J., 1999: Cloud-induced infrared radiative heating and its implications for large-scale tropical circulations. *J. Atmos. Sci.*, **56**, 2657–2672, doi:10.1175/1520-0469(1999)056<2657:CIIRHA>2.0.CO;2.

Stevens, B., S. Bony, and M. Webb, 2012: Clouds On-Off Klimate Intercomparison Experiment (COOKIE). 12 pp. [Available online at http://hdl.handle.net/11858/00-001M-0000-0024-580A-3.]

——, and Coauthors, 2013: Atmospheric component of the MPI-M Earth system model: ECHAM6. *J. Adv. Model. Earth Syst.*, **5**, 146–172, doi:10.1002/jame.20015.

Stuhlmann, R., and G. L. Smith, 1988a: A study of cloud-generated radiative heating and its generation of available potential energy. Part I: Theoretical background. *J. Atmos. Sci.*, **45**, 3911–3927, doi:10.1175/1520-0469(1988)045<3911:ASOCRH>2.0.CO;2.

——, and ——, 1988b: A study of cloud-generated radiative heating and its generation of available potential energy. Part II: Results for a climatological zonal mean January. *J. Atmos. Sci.*, **45**, 3928–3943, doi:10.1175/1520-0469(1988)045<3928:ASOCGR>2.0.CO;2.

Tian, B., 2015: Spread of model climate sensitivity linked to double–intertropical convergence zone bias. *Geophys. Res. Lett.*, **42**, 4133–4141, doi:10.1002/2015GL064119.

——, and V. Ramanathan, 2002: Role of tropical clouds in surface and atmospheric energy budget. *J. Climate*, **15**, 296–305, doi:10.1175/1520-0442(2002)015<0296:ROTCIS>2.0.CO;2.

——, and ——, 2003: A simple moist tropical atmosphere model: The role of cloud radiative forcing. *J. Climate*, **16**, 2086–2092, doi:10.1175/1520-0442(2003)016<2086:ASMTAM>2.0.CO;2.

——, G. J. Zhang, and V. Ramanathan, 2001: Heat balance in the Pacific warm pool atmosphere during TOGA COARE and CEPEX. *J. Climate*, **14**, 1881–1893, doi:10.1175/1520-0442(2001)014<1881:HBITPW>2.0.CO;2.

Voigt, A., and T. A. Shaw, 2015: Circulation response to warming shaped by radiative changes of clouds and water vapour. *Nat. Geosci.*, **8**, 102–106, doi:10.1038/ngeo2345.

——, S. Bony, J.-L. Dufresne, and B. Stevens, 2014: The radiative impact of clouds on the shift of the intertropical convergence zone. *Geophys. Res. Lett.*, **41**, 4308–4315, doi:10.1002/2014GL060354.

Voldoire, A., and Coauthors, 2013: The CNRM-CM5.1 global climate model: Description and basic evaluation. *Climate Dyn.*, **40**, 2091–2121, doi:10.1007/s00382-011-1259-y.

Wofsy, J., and Z. Kuang, 2012: Cloud-resolving model simulations and a simple model of an idealized Walker cell. *J. Climate*, **25**, 8090–8107, doi:10.1175/JCLI-D-11-00692.1.

Yukimoto, S., and Coauthors, 2012: A new global climate model of the Meteorological Research Institute: MRI-CGCM3: Model description and basic performance. *J. Meteor. Soc. Japan*, **90A**, 23–64, doi:10.2151/jmsj.2012-A02.

Zelinka, M., and D. Hartmann, 2010: Why is longwave cloud feedback positive? *J. Geophys. Res.*, **115**, D16117, doi:10.1029/2010JD013817.

Zhang, C., 2001: Double ITCZs. *J. Geophys. Res.*, **106**, 11 785–11 792, doi:10.1029/2001JD900046.

Zhang, Y.-C., and W. B. Rossow, 1997: Estimating meridional energy transports by the atmospheric and oceanic general circulations using boundary fluxes. *J. Climate*, **10**, 2358–2373, doi:10.1175/1520-0442(1997)010<2358:EMETBT>2.0.CO;2.